

AD-772 919

SENSITIVITY OF MATERIAL RESPONSE CALCULATIONS TO THE EQUATION OF STATE MODEL

William O. Wray

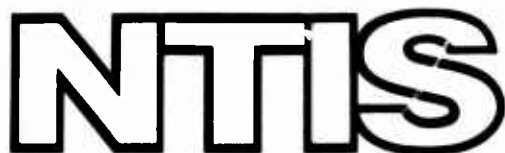
Systems, Science and Software

Prepared for:

Army Ballistic Research Laboratories

December 1973

DISTRIBUTED BY:



National Technical Information Service
U. S. DEPARTMENT OF COMMERCE
5285 Port Royal Road, Springfield Va. 22151

UNCLASSIFIED

Security Classification

AD772919

DOCUMENT CONTROL DATA - R & D

(Security classification of title, body of abstract and indexing annotation must be entered when the overall report is classified)

1. ORIGINATING ACTIVITY (Corporate author) Systems, Science and Software P.O. Box 1620 La Jolla, CA 92037	2a. REPORT SECURITY CLASSIFICATION Unclassified
2b. GROUP	

3. REPORT TITLE

Sensitivity of Material Response Calculations to the Equation of State Model

4. DESCRIPTIVE NOTES (Type of report and inclusive dates)

Final Report - May 73 - October 73

5. AUTHOR(S) (First name, middle initial, last name)

William O. Wray

6. REPORT DATE DECEMBER 1973	7a. TOTAL NO. OF PAGES 59	7b. NO. OF REFS 11
8a. CONTRACT OR GRANT NO. DAAD05-73-C-0489	9a. ORIGINATOR'S REPORT NUMBER(S) SSS-R-73-1910	
b. PROJECT NO. RDT&E Project 1W062105A659	9b. OTHER REPORT NO(S) (Any other numbers that may be assigned this report) BRL CONTRACT REPORT NO. 130	
c.		
d.		

10. DISTRIBUTION STATEMENT

Approved for public release; distribution unlimited.

11. SUPPLEMENTARY NOTES	12. SPONSORING MILITARY ACTIVITY US Army Ballistic Research Laboratories Aberdeen Proving Ground, MD 21005
-------------------------	--

13. ABSTRACT

This report examines the sensitivity of material response calculations to the choice of equation of state model. Three equation of state models, all of which are available as subroutines in the RIP code, are considered: 1) modified PUFF; 2) RIP mixed phase; and 3) GRAY. Each of these models is used to calculate the one-dimensional response of aluminum, beryllium and titanium; this series of calculations is performed for two distinct x-ray sources. The sensitivity of the calculated material response to the choice of equation of state model is characterized in terms of the generated impulse and the peak propagating stress at the time the radiation source is cut off. For the calculations presented in this report, the three equation of state models are in fairly good agreement.

Reproduced by
NATIONAL TECHNICAL
INFORMATION SERVICE
U. S. Department of Commerce
Springfield, VA 22151

66

DD FORM 1 NOV 64 1473 REPLACES DD FORM 1473, 1 JAN 64, WHICH IS
OBSOLETE FOR ARMY USE.

UNCLASSIFIED

Security Classification

UNCLASSIFIED

Security Classification

14 KEY WORDS	LINK A		LINK B		LINK C	
	ROLE	WT	ROLE	WT	ROLE	WT
Equation of State GRAY Equation of State RIP Mixed Phase Equation of State Modified PUFF Equation of State Aluminum Beryllium Titanium						

ia

UNCLASSIFIED

Security Classification

B A L L I S T I C R E S E A R C H L A B O R A T O R I E S

BRL CONTRACT REPORT NO. 130

SSS-R-73-1910

DECEMBER 1973

SENSITIVITY OF MATERIAL RESPONSE CALCULATIONS
TO THE EQUATION OF STATE MODEL

FINAL REPORT

William O. Wray
Systems, Science & Software
LaJolla, California

Contract No. DAAD05-73-C-0489
and
RDT&E Project No. 1W062105A659

Approved for public release; distribution unlimited.

A B E R D E E N P R O V I N G G R O U N D, M A R Y L A N D

" "

ABSTRACT

This report examines the sensitivity of material response calculations to the choice of equation of state model. Three equation of state models, all of which are available as subroutines in the RIP code, are considered: 1) modified PUFF; 2) RIP mixed phase; and 3) GRAY. Each of these models is used to calculate the one-dimensional response of aluminum, beryllium and titanium; this series of calculations is performed for two distinct x-ray sources. The sensitivity of the calculated material response to the choice of equation of state model is characterized in terms of the generated impulse and the peak propagating stress at the time the radiation source is cut off. For the calculations presented in this report, the three equation of state models are in fairly good agreement.

ACKNOWLEDGEMENT

This report and the associated research was supported by Contract No. DAAD05-73-C-0489 under the sponsorship of the Ballistic Research Laboratory in Aberdeen, Maryland. The project was funded and monitored through the efforts of Joseph F. Lacetera of the Effects Analysis Branch.

Mr. Robert A. Cecil and Mr. C. Michael Archuleta of the Systems, Science and Software (S³) scientific staff made significant technical contributions to the performance of the research and calculations reported herein. The EOSGEN code, which is currently undergoing refinement and documentation, is primarily the result of their efforts. Additionally, John R. Triplett, also a member of the S³ scientific staff, provided invaluable theoretical support by interpreting and evaluating the GRAY equation of state.

Preceding page blank

CONTENTS

	Page
1. INTRODUCTION	
1.1 OBJECTIVE AND PROCEDURE	1
1.2 EQUATION OF STATE MODELS	1
1.3 SOURCE DESCRIPTION	3
2. EQUATION OF STATE DATA	6
2.1 MODIFIED PUFF	6
2.2 RIP MIXED PHASE	6
2.3 GRAY	7
3. RESULTS AND DISCUSSION	26
4. CONCLUSIONS AND RECOMMENDATIONS	31
REFERENCES	36
APPENDIX A - THE EOSGEN CODE	37
A.1 THE VIRIAL EXPANSION	37
A.2 DEFINITION OF THE MIXED PHASE BOUNDARY	39
A.3 THE JOIN FUNCTION	42
APPENDIX B - CORRECTIONS TO EOS2	47
APPENDIX C - CORRECTIONS TO EOS3	50

Preceding page blank

LIST OF FIGURES

	Page
Figure 1. Incident energy spectrum for SPEC 1 radiation source (normalized to unity).	4
Figure 2. Normalized energy flux vs time for SPEC 1 radiation source.	5
Figure 3. Intersection of isotherms with mixed phase boundary.	32
Figure 4. Schematic pressure-volume diagram illustrating new join procedure for GRAY equation of state.	34
Figure A.1 Intersection of isotherms with mixed phase boundary.	40
Figure A.2 Schematic representation of the RIP mixed phase equation of state.	43
Figure B.1 Schematic representation of the RIP mixed phase equation of state.	48
Figure C.1 Schematic representation of GRAY EOS.	51

Preceding page blank

LIST OF TABLES

	Page
TABLE 1 Modified PUFF Parameters for Aluminum	8
TABLE 2 Modified PUFF Parameters for Beryllium	9
TABLE 3 Modified PUFF Parameters for Titanium	10
TABLE 4 EOSGEN Input Data for Aluminum	11
TABLE 5 EOSGEN Input Data for Beryllium	12
TABLE 6 EOSGEN Input Data for Titanium	13
TABLE 7 EOSGEN Output for Storage in /EQST/COMMON	14
TABLE 8 /EOSTAB/COMMON	15
TABLE 9 EOSTAB Input: Aluminum	17
TABLE 10 EOSTAB Input: Beryllium	19
TABLE 11 EOSTAB Input: Titanium	21
TABLE 12 Gray Equation of State Parameters for Aluminum	23
TABLE 13 Gray Equation of State Parameters for Beryllium	24
TABLE 14 Gray Equation of State Parameters for Titanium	25
TABLE 15 Summary of RIP Calculations	27
TABLE 16 Results of RIP Calculations on Aluminum	28
TABLE 17 Results of RIP Calculations on Beryllium	29
TABLE 18 Results of RIP Calculations on Titanium	30

Preceding page blank

1. INTRODUCTION

1.1 OBJECTIVE AND PROCEDURE

The purpose of this report is to determine the sensitivity of material response calculations to the choice of equation of state model. Three equation of state models, all of which are available as subroutines in the RIP^[1] code, are considered: 1) modified PUFF; 2) RIP mixed phase; 3) GRAY. Each of these models is used to calculate the one-dimensional response of aluminum, beryllium and titanium; this series of calculations is performed for two distinct x-ray sources. The sensitivity of the calculated material response to the choice of equation of state model is characterized in terms of the generated impulse and the peak propagating stress at the time the radiation source is cut off. Whenever possible, handbook values are used for the required equation of state data; no attempt was made to adjust the data in order to reduce the differences between the three models.

1.2 EQUATION OF STATE MODELS

The first equation of state considered in this report is referred to as the modified PUFF equation of state.^[1] The modified PUFF equation of state is the simplest of the three models; it consists of a Mie-Gruneisen solid equation of state for the compressed region which is joined at the ambient density to a function which limits to an ideal gas equation of state as the density approaches zero. Pressure continuity is maintained at the ambient density for all energies, but the sound speed is continuous only at the zero reference energy; the discontinuity in sound speed becomes more severe as the energy is increased.

The RIP mixed phase equation of state is based on a virial expansion which was applied by Tuerpe, Keeler and McCarthy^[2] to the study of aluminum at high temperature and pressure. The equation of state was later generalized to other metals by D. Steinberg and reported in an internal memo dated August 22, 1967 at Lawrence Livermore Laboratory. Incorporation of the Steinberg equation of state into the RIP code involved the following tasks:

1. The caloric equation of state was inverted and the resulting expression for the temperature was substituted into the thermal

equation of state, thereby yielding a formula for the pressure as a function of energy and density. Seven independent coefficients appear in this formula and they are evaluated by the EOSGEN* code and subsequently input to EOSTAB common in the RIP code.

2. A Maxwell construction was required in order to determine corresponding values of pressure, energy, sound speed and density on the mixed phase boundary. This task is also performed by the EOSGEN code, and points on the mixed phase boundary are subsequently input to EOSTAB common in the RIP code.
3. A join function was developed which provides for pressure and sound speed continuity between the virial expansion for expanded states and the Mie-Gruneisen solid equation of state for the compressed region. The coefficients in the join function are evaluated by the EOSGEN code and subsequently input to EQST common in the RIP code.

A brief discussion of the EOSGEN code and associated corrections** to the EOS2 subroutine in the RIP code is presented in Appendix A. All of the work presented in Appendix A was performed in support of Contract DAAD05-73-C-0489 and was required in order to perform hydrodynamic calculations using the RIP mixed phase equation of state in the RIP code.

The third equation of state considered in this research is the GRAY three-phase equation of state for metals developed by E.B. Royce[3] at Lawrence Livermore Laboratory. Material near normal density, in the solid-liquid region, is described by a scaling-law equation of state for metals developed by Grover.[4] The scaling-law equation of state includes a Gruneisen description of the solid[5] normalized to the experimental Hugoniot. Material in the liquid-vapor region is treated according to an equation of state developed by Young and Alder;[6] their van der Waals model uses an analytic representation of the classical hard-sphere equation of state with a van der Waals attractive term added. The complete equation

* Documentation of the EOSGEN code is in progress.

** It was necessary to develop a new join function in order to allow pressure and sound speed continuity between the compressed and expanded equations of state.

of state, as described in Reference 3, is developed by analytically joining the Grover scaling law and the Young-Alder models at a volume in the range 1.3 to 1.5 times normal volume. This is accomplished by adding correction terms to the Young-Alder equation of state employed on the low density side of the join volume.

It was necessary to make several corrections to the EOS3 subroutine in the RIP code before performing calculations with the GRAY equation of state. These corrections are presented in Appendix B.

1.3 SOURCE DESCRIPTIONS

The first radiation source (SPEC 1) was prescribed by the Ballistic Research Laboratory.[7] The energy spectrum and the time dependence of the energy flux are presented in Figure 1 and Figure 2 respectively. The second peak in the energy spectrum is due to a typographical error in Reference 7. The calculations were performed before this error was recognized, but since the same spectrum was used throughout, the calculations still represent a valid sensitivity study. A fluence level of 5952 cal/cm² was used for all calculations performed with this radiation source.

The second radiation source (SPEC 2) considered in this study is a 2-keV blackbody with a 10-nsec square pulse shine time. Appropriate fluence levels were selected in order to guarantee that several zones of material are vaporized at the front surface of each metal considered. The fluence levels selected are:

Aluminum:	100 cal/cm ²
Beryllium:	2000 cal/cm ²
Titanium:	100 cal/cm ²

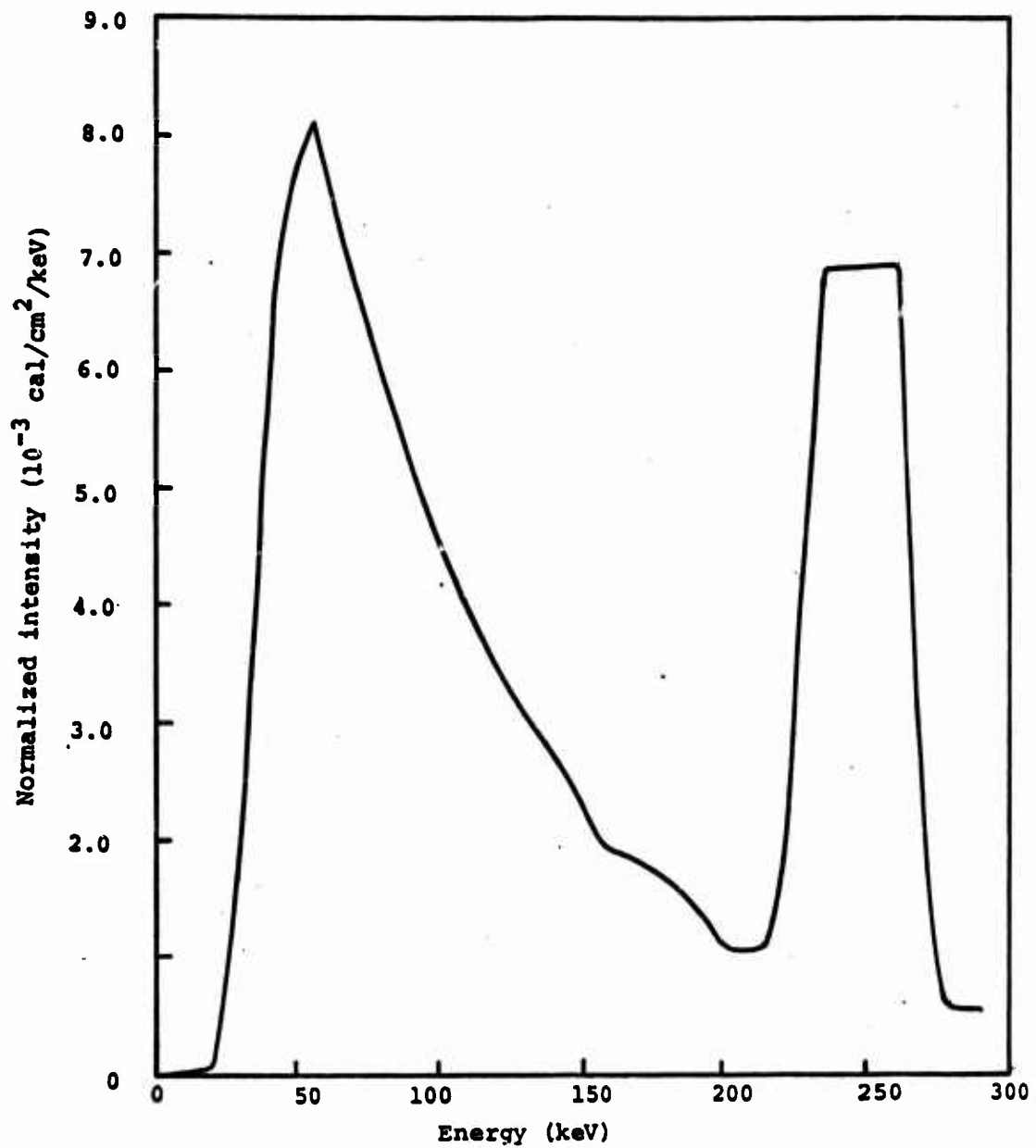


Figure 1. Incident energy spectrum for SPEC 1 radiation source (normalized to unity).

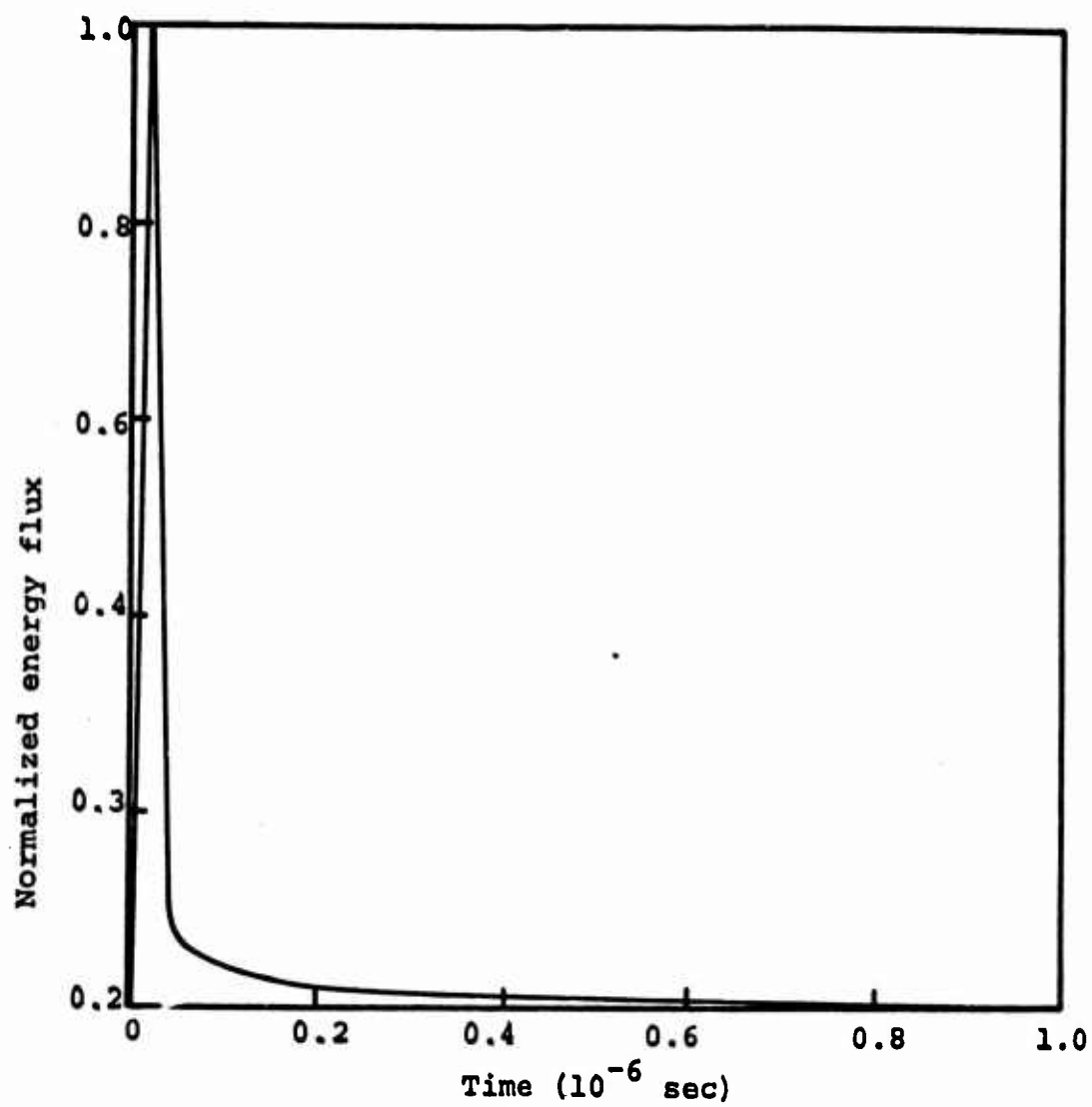


Figure 2. Normalized energy flux vs time for SPEC 1 radiation source.

2.1 MODIFIED PUFF

The modified PUFF equation of state parameters for aluminum, beryllium, and titanium are presented in Tables 1, 2, and 3 respectively. All of the parameters appearing in the tables were obtained from Reference 8 with the exceptions of E_{LV} , E_{LM} , and E_{SM} which were calculated as described in the following paragraph.

The incipient melt energy, E_{SM} , is obtained by multiplying the difference between the melt temperature (Reference 9, page D-103) and the reference temperature, 20° C, by the heat capacity at constant pressure (Reference 9, D-97). The complete melt energy, E_{LM} , is obtained by adding the heat of fusion (Reference 10) to the incipient melt energy. Finally, an approximate value for the incipient vaporization energy, E_{LV} , is obtained by multiplying the difference between the melt temperature and the boiling temperature (Reference 9, page D-103) by the heat capacity and adding the result to the complete melt energy. These three energy parameters are used for the momentum edits (the momentum of each thermodynamic state is displayed) and for determining the energy density, E_{SM} , at which the material should have zero strength. All of the data for modified PUFF is stored in the ESTCON array in EQST common.

2.2 RIP MIXED PHASE

The first thirteen parameters listed in Tables 1, 2, and 3 are required as input to EQST common in order to apply the EOS2 equation of state subroutine in hydrodynamic calculations on aluminum, beryllium and titanium, respectively. The remaining equation of state data are generated by the EOSGEN code which is described in Appendix A.

Fundamental material properties of aluminum, beryllium, and titanium which are required as input data to the EOSGEN code are presented in Tables 4, 5, and 6 respectively. The ambient densities are the same values used for the modified PUFF equation of state and the reference temperature for all three materials is assumed to be 300° K. The bulk modulus

of aluminum was calculated according to the relation

$$\beta_0 = \frac{Y}{3(1-2\sigma)} ,$$

where β_0 is the bulk modulus, Y is Young's modulus and σ is Poisson's ratio. Numerical values for Y and σ were obtained from Table 3.1 on page 44 of Reference 1. The bulk moduli of beryllium and titanium were taken equal to the linear Hugoniot coefficients, A_1 , used in the modified PUFF equation of state. Constant pressure heat capacities obtained from page D-97 of Reference 9 were used for c_{v0} , the constant volume heat capacity at the reference state; heat capacities at constant pressure and volume are almost identical for solids at low temperatures. The critical pressure, temperature, and volume of aluminum were obtained from Table 3.1 on page 44 of Reference 1. The critical points of beryllium and titanium were calculated using a procedure presented in Reference 6. The required relations are

$$v_c = (2.417 \times 10^{24}) \sigma^3 ,$$

$$T_c = \frac{.7232 a_y}{R v_c} ,$$

$$P_c = \frac{.2596 a_y}{v_c^2} ,$$

where v_c , T_c , and P_c are the critical volume, temperature, and pressure, respectively, σ is the hard sphere diameter, a_y is the coefficient of the attractive potential for the vapor, and R is the universal gas constant. The hard sphere diameter is related to the excluded volume, V_b , by the equation

$$\sigma^3 = \frac{6V_b}{\pi N} ,$$

where N is Avogadro's number. Numerical values of a_y and V_b are presented in Table 3.2 on page 52 of Reference 1.

2.3 GRAY

The GRAY equation of state parameters for aluminum, beryllium, and titanium are presented in Tables 11, 12 and 13 respectively; the parameters also used in the modified PUFF equation of state are not repeated in these tables. The entropies of melting were obtained from Reference 9; all other GRAY equation of state parameters were obtained from the original Lawrence Livermore Laboratories report by E.B. Royce.[5]

TABLE 1
MODIFIED PUFF PARAMETERS FOR ALUMINUM

Property	Symbol	Numerical Value
Ambient Density	ρ_0	2.7 gm/cm ³
Gruneisen coefficient	G_0	2.09
Coefficient of linear term in cubic fit to the Hugoniot	A_1	7.99×10^{11} dynes/cm ²
Coefficient of quadric term in cubic fit to the Hugoniot	A_2	1.139×10^{12} dynes/cm ²
Coefficient of cubic term in cubic fit to the Hugoniot	A_3	1.398×10^{12} dynes/cm ²
Bulk sound speed	C_0	5.44×10^5 cm/sec
Shear modulus	AMU	2.561×10^{11} dynes/cm ²
Yield strength	γ_0	5.0×10^9 dynes/cm ²
Sublimation energy	E_{VV}	1.177×10^{11} ergs/cm
Incipient vaporization energy	E_{LV}	2.65×10^{10} ergs/gm
Complete melt energy	E_{LM}	9.7×10^9 ergs/gm
Incipient melt energy	E_{SM}	5.77×10^9 ergs/gm
Perfect gas constant	H	.6667
Fairing constant	N	1.203

TABLE 2
MODIFIED PUFF PARAMETERS FOR BERYLLIUM

Property	Symbol	Numerical Value
Ambient density	ρ_o	1.851 gm/cm ³
Gruneisen coefficient	G_o	1.45
Coefficient of linear term in cubic fit to the Hugoniot	A_1	1.208×10^{12} dynes/cm ²
Coefficient of quadratic term in cubic fit to the Hugoniot	A_2	1.529×10^{12} dynes/cm ²
Coefficient of cubic term in cubic fit to the Hugoniot	A_3	4.63×10^{11} dynes/cm ²
Bulk sound speed	C_o	8.08×10^5 cm/sec
Shear modulus	AMU	1.46×10^{12} dynes/cm ²
Yield strength	Y_o	3.10×10^9 dynes/cm ²
Sublimation energy	E_{VV}	3.549×10^{11} ergs/gm
Incipient vaporization energy	E_{LV}	6.67×10^{10} ergs/gm
Complete melt energy	E_{SM}	3.59×10^{10} ergs/gm
Incipient melt energy	H	2.29×10^{10} ergs/gm
Perfect gas constant		.6667
Fairing constant	N	1.266

TABLE 3
MODIFIED PUFF PARAMETERS FOR TITANIUM

Property	Symbol	Numerical Value
Ambient density	ρ_0	4.51 gm/cm ³
Gruneisen coefficient	G_0	2.04
Coefficient of linear term in cubic fit to the Hugoniot	A_1	9.94×10^{11} dynes/cm ²
Coefficient of quadratic term in cubic fit to the Hugoniot	A_2	1.249×10^{12} dynes/cm ²
Coefficient of cubic term in cubic fit to the Hugoniot	A_3	4.897×10^{11} dynes/cm ²
Bulk sound speed	C_0	4.7×10^5 cm/sec
Shear modulus	AMU	4.404×10^{11} dynes/cm ²
Yield strength	γ_0	1.38×10^9 dynes/cm ²
Sublimation energy	E_{VV}	9.683×10^{10} ergs/gm
Incipient vaporization energy	E_{LV}	2.019×10^{10} ergs/gm
Complete melt energy	E_{LM}	1.189×10^{10} ergs/gm
Incipient melt energy	E_{SM}	8.66×10^9 ergs/gm
Perfect gas constant	H	.6667
Fairing constant	N	1.114

TABLE 4
EOSGEN INPUT DATA FOR ALUMINUM

Property	Symbol	Numerical Value
Ambient density	ρ_o	2.7 gm/cm ³
Ambient temperature	θ_o	300°K
Bulk modulus at reference state	$A_1(\beta_o)$	6.75×10^{11} dynes/cm ²
Heat capacity at reference state	c_{vo}	9.0×10^6 ergs/gm °K
Critical pressure	p_c	5.3×10^9 dynes/cm ²
Critical temperature	θ_c	11,400°K
Critical volume	v_c	2.7 cm ³ /gm

TABLE 5
EOSGEN INPUT DATA FOR BERYLLIUM

Property	Symbol	Numerical Value
Ambient Density	ρ_o	1.851 gm/cm ³
Ambient temperature	θ_o	300°K
Bulk modulus at reference state	$A_1(\beta_o)$	1.208×10 ¹² dynes/cm ²
Heat capacity at reference state	c_{vo}	1.82×10 ⁷ ergs/gm °K
Critical Pressure	P_c	1.8×10 ¹⁰ dynes/cm ²
Critical temperature	θ_c	11,400°K
Critical volume	v_c	2.03 cm ³ /gm

TABLE 6
EOSGEN INPUT DATA FOR TITANIUM

Property	Symbol	Numerical Value
Ambient density	ρ_o	4.51 gm/cm ³
Ambient temperature	θ_o	300°K
Bulk modulus at reference state	$A_1(\beta_o)$	9.94×10 ¹¹ dynes/cm ²
Heat capacity at reference state	c_{vo}	5.23×10 ⁶ ergs/gm °K
Critical pressure	P_c	7.98×10 ⁹ dynes/cm ²
Critical temperature	θ_c	12,550°K
Critical volume	V_c	0.984 cm ³ /gm

TABLE 7
EOSGEN OUTPUT FOR STORAGE IN /EQST/COMMON

Numerical Value For:			
Property	Symbol	Aluminum	Beryllium
Cut-off density	ρ_{CO} gm/cm ³	2.0115	1.842
Coefficients	$c_1 \frac{\text{dynes}}{\text{cm}^2}$	2.642×10^{-12}	9.695×10^{-14}
of	$c_2 \frac{\text{dynes/cm}^2}{\text{gm/cm}^3}$	-3.746×10^{-12}	-1.576×10^{-15}
the	$c_3 \frac{\text{dynes/cm}^2}{\text{gm/cm}^3}$	1.595×10^{-12}	8.538×10^{-14}
join	$c_4 \frac{\text{dynes/cm}^2}{\text{gm/cm}^3}$	-2.111×10^{-11}	-1.541×10^{-14}
functions	$c_5 (C_A)$ gm/cm ³	5.643	3.869
	$c_6 (C_B)$ gm/cm ³	2.681	-5.754
	$c_7 (C_C)$ gm/cm ³	-2.700	3.834
			9.426
			-12.78
			8.517

TABLE 8
 /EOSTAB/COMMON

Purpose: Stores the constants and the tabular values which describe the mixed phase region in the RIP mixed-phase equation of state model.

Used In: CARDS, DREAD, EDIT, EOS2, RIP, SPRINT

Variable	Location	Definition
THETA(I) I=1,100	Y1	Temperature ($^{\circ}$ K) of the points for the mixed phase region table. Listed in ascending order from $T = 0$ to $T = T_{crit}$. These values are determined by the EOSGEN code and are not used in subroutine EOS2.
PU(I) I=1,100	Y101	Pressure (dynes/cm ²) of the points in the mixed phase region table. These values correspond to THETA values and are in ascending order from $P = 0$ to $P = P_{crit}$.
RHOU(I) I=1,100	Y201	Density (g/cm ³) of the points for the range $\rho_{co} > \rho > \rho_{crit}$ of the mixed phase region: the variable ρ_{co} is the value of the density at the cut-off point for the mixed phase region which is entered into ESTCON(16,N). The variable ρ_{crit} corresponds to the density at P_{crit} . These values correspond to the values appearing in the PU(I) array.
EU(I) I=1,100	Y301	Specific internal energy (erg/g) corresponding to the points in the RHOU(I) array.

TABLE 8, /EOSTAB/COMMON (Continued)

Variable	Location	Definition
CU(I) I=1,100	Y401	Sound speed (cm/sec) corresponding to the points in the RHOU(I) array.
RHOL(U) I=1,100	Y501	Density (g/cm^3) of the points for the range $\rho_{\text{crit}} > \rho > 0$ of the mixed phase region. These values correspond to the values appearing in the PU(I) array.
EL(I) I=1,100	Y601	Specific internal energy (erg/g) corresponding to the points in the RHOL(I) array.
CL(I) I=1,100	Y701	Sound speed (cm/sec) corresponding to the points in the RHOL(I) array.
Z(I) I=1,15	Y801	Z(1) through Z(8) are defined in the EOSGEN code. These are coefficients used in the calculation of pressures and sound speeds for state points above and below the mixed phase region. Z(9) through Z(15) are coefficients calculated within subroutine EOS2 and are used for state points above and below the mixed phase.

TABLE 9
EOSTAB INPUT: ALUMINUM

$\gamma_1 =$

3.0000+02, 1.8540+03, 2.0760+03, 2.2980+03, 2.5200+03,
 2.7420+03, 2.9643+03, 3.1360+03, 3.4033+03, 3.6300+03,
 3.8520+03, 4.0740+03, 4.2960+03, 4.5180+03, 4.7400+03,
 4.9620+03, 5.1840+03, 5.4160+03, 5.6230+03, 5.8500+03,
 6.0720+03, 6.2940+03, 6.5160+03, 6.7380+03, 6.9600+03,
 7.1620+03, 7.4040+03, 7.6260+03, 7.8480+03, 8.0700+03,
 8.2920+03, 8.5140+03, 8.7360+03, 8.9580+03, 9.1800+03,
 9.4020+03, 9.6240+03, 9.8360+03, 1.0069+04, 1.0293+04,
 1.0512+04, 1.0734+04, 1.0956+04, 1.1178+04,
 1.1400+04

$\gamma_{101} =$

3.0000, 1.5397+03, 1.1142+04, 5.4833+04, 2.3249+05,
 5.9992+05, 1.5005+06, 3.2346+06, 6.4628+06, 1.1663+07,
 1.9608+07, 3.1378+07, 4.6368+07, 6.7821+07, 9.4657+07,
 1.2820+08, 1.6902+08, 2.1787+08, 2.7518+08, 3.4146+08,
 4.1714+08, 5.0253+08, 5.9796+08, 7.0356+08, 8.1961+08,
 9.4614+08, 1.0833+09, 1.2310+09, 1.3895+09, 1.5566+09,
 1.7392+09, 1.9283+09, 2.1299+09, 2.3398+09, 2.5629+09,
 2.7920+09, 3.0330+09, 3.2838+09, 3.5444+09, 3.8144+09,
 4.0935+09, 4.3819+09, 4.6792+09, 4.9853+09,
 5.3000+09

$\gamma_{231} =$

2.7000+00, 2.1086+00, 2.0425+00, 1.9799+00, 1.9202+00,
 1.8634+00, 1.8391+00, 1.7570+00, 1.7371+00, 1.6592+00,
 1.6131+00, 1.5687+00, 1.5257+00, 1.4843+00, 1.4444+00,
 1.4051+00, 1.3672+00, 1.3304+00, 1.2946+00, 1.2596+00,
 1.2254+00, 1.1920+00, 1.1593+00, 1.1272+00, 1.0957+00,
 1.0647+00, 1.0341+00, 1.0040+00, 9.7415-01, 9.4461-01,
 9.1525-01, 8.8604-01, 8.5689-01, 8.2771-01, 7.9841-01,
 7.6885-01, 7.3886-01, 7.0327-01, 6.7635-01, 6.4420-01,
 6.0975-01, 5.7260-01, 5.3090-01, 4.8003-01,
 3.7037-01

$\gamma_{301} =$

3.0000, 2.2583+10, 2.6249+10, 2.9961+10, 3.3737+10,
 3.7480+10, 4.1273+10, 4.5079+10, 4.8895+10, 5.2715+10,
 5.6536+10, 6.0357+10, 6.4178+10, 6.7992+10, 7.1908+10,
 7.5613+10, 7.9419+10, 8.3216+10, 8.7005+10, 9.0800+10,
 9.4587+10, 9.8371+10, 1.0215+11, 1.0594+11, 1.0972+11,
 1.1350+11, 1.1729+11, 1.2109+11, 1.2490+11, 1.2871+11,
 1.3255+11, 1.3643+11, 1.4028+11, 1.4418+11, 1.4813+11,
 1.5211+11, 1.5616+11, 1.6028+11, 1.6446+11, 1.6861+11,
 1.7330+11, 1.7803+11, 1.8315+11, 1.8933+11,
 1.9969+11

$\gamma_{431} =$

5.0000+05, 4.3552+05, 4.2724+05, 4.1913+05, 4.1116+05,
 4.0331+05, 3.9555+05, 3.9787+05, 3.8024+05, 3.7263+05,
 3.6518+05, 3.5771+05, 3.5024+05, 3.4264+05, 3.3535+05,
 3.2799+05, 3.2054+05, 3.1313+05, 3.0569+05, 2.9921+05,

TABLE 9, EOSTAB INPUT: ALUMINUM (Continued)

	2.9370+05, 2.8316+35, 2.7558+05, 2.6794+35, 2.6025+35,
	2.5249+05, 2.4464+05, 2.3672+05, 2.2871+05, 2.2059+05,
	2.1233+05, 2.0395+35, 1.9542+05, 1.8673+35, 1.7785+05,
	1.6876+05, 1.5942+05, 1.4982+05, 1.3993+05, 1.2970+05,
	1.1939+05, 1.0809+35, 9.6729+04, 8.5334+04,
	7.8535+04
Y501=	0.0000 , 2.1913-07, 1.4248-C6, 6.3441-C8, 2.1341-05,
	5.8130-35, 1.3459-34, 2.7439-34, 5.0335-34, 8.5857-34,
	1.3646-03, 2.0534-C3, 2.9516-03, 4.0860-C3, 5.4743-C3,
	7.1471-03, 9.0930-33, 1.11354-32, 1.3929-32, 1.5031-32,
	2.0069-02, 2.3654-C2, 2.7595-02, 3.1902-02, 3.6589-C2,
	4.1667-02, 4.7150-02, 5.3761-32, 5.9412-32, 6.6253-02,
	7.3595-02, 8.1479-C2, 8.9958-C2, 9.9091-C2, 1.0896-C1,
	1.1965-01, 1.3129-01, 1.4405-01, 1.5819-01, 1.7404-01,
	1.9213-01, 2.1336-01, 2.3957-01, 2.7539-C1,
	3.7037-01
Y601=	1.3194+11, 1.4592+11, 1.4792+11, 1.4932+11, 1.5192+11,
	1.5391+11, 1.5500+11, 1.5789+11, 1.5986+11, 1.6182+11,
	1.6378+11, 1.6571+11, 1.6763+11, 1.6952+11, 1.7139+11,
	1.7323+11, 1.7505+11, 1.7684+11, 1.786C+11, 1.8033+11,
	1.8233+11, 1.8370+11, 1.8533+11, 1.8633+11, 1.8853+11,
	1.9004+11, 1.9153+11, 1.9299+11, 1.9441+11, 1.9579+11,
	1.9712+11, 1.9841+11, 1.9964+11, 2.0082+11, 2.0134+11,
	2.0798+11, 2.0395+11, 2.0482+11, 2.0557+11, 2.0619+11,
	2.3661+11, 2.0578+11, 2.0554+11, 2.0551+11,
	1.9969+11
Y701=	3.3612+04, 9.9676+C4, 1.0531+05, 1.1078+C5, 1.1600+C5,
	1.2096+05, 1.257J+35, 1.3320+05, 1.3436+35, 1.3849+05,
	1.4227+05, 1.4578+05, 1.4904+05, 1.52L3+05, 1.5475+C5,
	1.5720+05, 1.5937+05, 1.6127+05, 1.629J+05, 1.6426+05,
	1.6575+05, 1.6617+05, 1.6673+05, 1.6702+05, 1.6704+05,
	1.6679+C5, 1.6623+35, 1.6548+05, 1.6491+35, 1.6305+05,
	1.6140+05, 1.5444+C5, 1.5715+05, 1.5453+C5, 1.5153+C5,
	1.4814+C5, 1.4433+05, 1.4382+05, 1.3515+35, 1.2964+05,
	1.2335+05, 1.1605+C5, 1.0740+05, 9.6593+C4,
	7.8535+04
Y801=	3.7658+C6,-2.0254+36,-9.2322+10, 6.2997+36, 3.2563+10,
	9.0000+06, 1.2924+11, 4.5000+C1, 0.0000 , 0.0000 ,
	-5.4376+10,-2.4900+10,-8.5331+10, 6.8584+10,-1.1386+10

TABLE 10

EOSTAB INPUT: BERYLLIUM

Y1=

3.0000+02, 2.0780+03, 2.2980+03, 2.5200+03, 2.7420+03,
 4.0740+03, 4.2980+03, 4.5180+03, 4.7400+03, 4.9620+03,
 5.1840+03, 5.4060+03, 5.6280+03, 5.8500+03, 6.0720+03,
 6.2940+03, 6.5160+03, 6.7380+03, 6.9600+03, 7.1820+03,
 7.4040+03, 7.6260+03, 7.8480+03, 8.0700+03, 8.2920+03,
 8.5140+03, 8.7360+03, 8.9580+03, 9.1800+03, 9.4020+03,
 9.6240+03, 9.8460+03, 1.0068+04, 1.0290+04, 1.0512+04,
 1.0734+04, 1.0956+04, 1.1178+04,
 1.1400+04

Y131=

0.0000, 3.4925+03, 1.9072+04, 7.9035+04, 2.6176+05,
 7.2837+05, 1.7635+06, 3.8236+06, 7.5545+06, 1.3852+07,
 2.3831+07, 3.8866+07, 6.0556+07, 9.0727+07, 1.3139+08,
 1.8475+08, 2.5312+08, 3.3399+08, 4.4493+08, 5.7360+08,
 7.2773+08, 9.1011+08, 1.1235+09, 1.3706+09, 1.6549+09,
 1.9799+09, 2.3454+09, 2.7574+09, 3.2133+09, 3.7303+09,
 4.2973+09, 4.9212+09, 5.6060+09, 6.3540+09, 7.1684+09,
 8.0526+09, 9.0093+09, 1.0042+10, 1.1153+10, 1.2346+10,
 1.3624+10, 1.4990+10, 1.6448+10,
 1.8000+10

Y201=

1.8510+00, 1.7476+00, 1.7337+00, 1.7195+00, 1.7051+00,
 1.6903+00, 1.6753+00, 1.6601+00, 1.6445+00, 1.6285+00,
 1.6123+00, 1.5957+00, 1.5787+00, 1.5613+00, 1.5436+00,
 1.5254+00, 1.5068+00, 1.4878+00, 1.4683+00, 1.4483+00,
 1.4278+00, 1.4067+00, 1.3351+00, 1.3629+00, 1.3399+00,
 1.3164+00, 1.2921+00, 1.2669+00, 1.2410+00, 1.2141+00,
 1.1863+00, 1.1572+00, 1.1270+00, 1.0954+00, 1.0622+00,
 1.0272+00, 9.9011-01, 9.5044-01, 9.0764-01, 8.6069-01,
 8.3834-01, 7.4667-01, 6.6873-01,
 4.9261-01

Y301=

0.0000, 3.3674+10, 3.8054+10, 4.2478+10, 4.6948+10,
 5.1469+10, 5.6042+10, 6.0569+10, 6.5355+10, 7.3102+10,
 7.4915+10, 7.9797+10, 8.4752+10, 8.9785+10, 9.4900+10,
 1.0010+11, 1.0540+11, 1.1179+11, 1.1630+11, 1.2191+11,
 1.2764+11, 1.3351+11, 1.3951+11, 1.4566+11, 1.5198+11,
 1.5806+11, 1.6514+11, 1.7232+11, 1.7912+11, 1.8647+11,
 1.9408+11, 2.0201+11, 2.1026+11, 2.1890+11, 2.2798+11,
 2.3756+11, 2.4773+11, 2.5862+11, 2.7039+11, 2.8333+11,
 2.9781+11, 3.1472+11, 3.3615+11,
 3.8379+11

Y401=

3.3785+05, 7.3785+05, 7.2362+05, 7.1927+05, 7.0979+05,
 7.0014+05, 6.9037+05, 6.8046+05, 6.7039+05, 6.6017+05,
 6.4975+05, 6.3917+05, 6.2840+05, 6.1745+05, 6.0631+05,
 5.9496+05, 5.8341+05, 5.7164+05, 5.5965+05, 5.4743+05,
 5.3497+05, 5.2228+05, 5.0930+05, 4.9635+05, 4.8254+05.

TABLE 10, EOSTAB INPUT: BERYLLIUM (Continued)

4.3375×10^5 , 4.5463×10^5 , 4.4319×10^5 , 4.2545×10^5 , 4.1033×10^5 ,
 3.9483×10^5 , 3.7892×10^5 , 3.6263×10^5 , 3.4538×10^5 , 3.2865×10^5 ,
 3.1093×10^5 , 2.9269×10^5 , 2.7391×10^5 , 2.5453×10^5 , 2.3483×10^5 ,
 2.1468×10^5 , 1.9466×10^5 , 1.7614×10^5 ,
 1.7141×10^5

V501=

3.0000 , 1.7140×10^{-3} , 8.6264×10^{-7} , 3.2815×10^{-6} , 9.9299×10^{-6} ,
 2.5552×10^{-5} , 5.7596×10^{-5} , 1.1671×10^{-4} , 2.1685×10^{-4} , 3.7511×10^{-4} ,
 5.1127×10^{-4} , 9.4752×10^{-4} , 1.4378×10^{-3} , 2.0175×10^{-3} , 2.8030×10^{-3} ,
 3.7915×10^{-3} , 5.0110×10^{-3} , 6.4901×10^{-3} , 8.2582×10^{-3} , 1.0346×10^{-2} ,
 1.2735×10^{-2} , 1.5608×10^{-2} , 1.8349×10^{-2} , 2.2378×10^{-2} , 2.6745×10^{-2} ,
 3.1489×10^{-2} , 3.6823×10^{-2} , 4.2807×10^{-2} , 4.9509×10^{-2} , 5.6991×10^{-2} ,
 6.5354×10^{-2} , 7.4584×10^{-2} , 8.5120×10^{-2} , 9.6737×10^{-2} , 1.0993×10^{-1} ,
 1.2469×10^{-1} , 1.4146×10^{-1} , 1.6064×10^{-1} , 1.8237×10^{-1} , 2.0906×10^{-1} ,
 2.4078×10^{-1} , 2.8112×10^{-1} , 3.3781×10^{-1} ,
 4.0261×10^{-1}

V631=

3.3541×10^1 , 3.6774×10^1 , 3.7178×10^1 , 3.7582×10^1 , 3.7985×10^1 ,
 3.8389×10^1 , 3.8792×10^1 , 3.9194×10^1 , 3.9574×10^1 , 3.9902×10^1 ,
 4.0388×10^1 , 4.0780×10^1 , 4.1167×10^1 , 4.1550×10^1 , 4.1925×10^1 ,
 4.2294×10^1 , 4.2654×10^1 , 4.3335×10^1 , 4.3345×10^1 , 4.3675×10^1 ,
 4.3993×10^1 , 4.4296×10^1 , 4.4585×10^1 , 4.4857×10^1 , 4.5112×10^1 ,
 4.5349×10^1 , 4.5565×10^1 , 4.5758×10^1 , 4.5927×10^1 , 4.6070×10^1 ,
 4.6184×10^1 , 4.6265×10^1 , 4.6310×10^1 , 4.6315×10^1 , 4.6274×10^1 ,
 4.6430×10^1 , 4.3596×10^1 , 4.2700×10^1 ,
 3.8379×10^1

V701=

5.3710×10^4 , 1.7529×10^5 , 1.8379×10^5 , 1.9244×10^5 , 2.0372×10^5 ,
 2.0866×10^5 , 2.1628×10^5 , 2.2259×10^5 , 2.3061×10^5 , 2.3732×10^5 ,
 2.4374×10^5 , 2.4985×10^5 , 2.5554×10^5 , 2.6111×10^5 , 2.6625×10^5 ,
 2.7105×10^5 , 2.7550×10^5 , 2.7959×10^5 , 2.8332×10^5 , 2.8668×10^5 ,
 2.8966×10^5 , 2.9225×10^5 , 2.9145×10^5 , 2.9624×10^5 , 2.9762×10^5 ,
 2.9858×10^5 , 2.9909×10^5 , 2.9915×10^5 , 2.9873×10^5 , 2.9782×10^5 ,
 2.9637×10^5 , 2.9438×10^5 , 2.9177×10^5 , 2.8352×10^5 , 2.8456×10^5 ,
 2.7980×10^5 , 2.7415×10^5 , 2.6747×10^5 , 2.5955×10^5 , 2.5014×10^5 ,
 2.3882×10^5 , 2.2481×10^5 , 2.0544×10^5 ,
 1.7141×10^5

V831=

9.6156×10^6 , 1.1997×10^7 , -3.5529×10^6 , -3.6706×10^6 , 1.9242×10^6 ,
 -1.7433×10^6 , -3.8696×10^6 , 4.4197×10^6 , -1.3538×10^6 , 1.9404×10^6

TABLE 11
EOSTAB INPUT: TITANIUM

```

    V1=          3.0000+02, 3.2400+03, 3.4850+03, 3.7300+03, 3.9750+03,
    4.2230+03, 4.4650+03, 4.7100+03, 4.9550+03, 5.2000+03,
    5.4450+03, 5.6900+03, 5.9350+03, 6.1800+03, 6.4250+03,
    6.6700+03, 6.9150+03, 7.1600+03, 7.4050+03, 7.6500+03,
    7.8950+03, 8.1400+03, 8.3850+03, 8.6300+03, 8.8750+03,
    9.1230+03, 9.3650+03, 9.6100+03, 9.8550+03, 1.0100+04,
    1.0345+04, 1.0590+04, 1.0835+04, 1.1080+04, 1.1325+04,
    1.1570+04, 1.1815+04, 1.2060+04, 1.2315+04,
    1.2550+04

    V131=        0.0000, 2.8880+03, 1.1178+04, 3.6741+04, 1.0452+05,
    2.6386+05, 6.0264+35, 1.2645+06, 2.4685+06, 4.5287+06,
    7.8730+06, 1.3061+07, 2.0795+07, 3.1934+07, 4.7501+07,
    6.8681+07, 9.6826+07, 1.3346+08, 1.8025+08, 2.3931+08,
    3.1176+08, 4.0065+08, 5.0785+08, 6.3590+08, 7.8723+08,
    9.5461+08, 1.1737+09, 1.4487+09, 1.6814+09, 1.9910+09,
    2.3438+09, 2.7404+09, 3.1854+09, 3.6823+09, 4.2350+09,
    4.8474+09, 5.5233+09, 6.2583+09, 7.0856+09,
    7.9800+09

    V231=        4.5100+00, 4.1080+00, 4.0703+00, 4.0318+00, 3.9925+00,
    3.9525+00, 3.9115+00, 3.8597+00, 3.8259+00, 3.7831+00,
    3.7382+00, 3.6923+00, 3.6452+00, 3.5969+00, 3.5473+00,
    3.4954+00, 3.4441+00, 3.3903+00, 3.3350+00, 3.2779+00,
    3.2190+00, 3.1584+00, 3.0956+00, 3.0307+00, 2.9634+00,
    2.8936+00, 2.8210+00, 2.7354+00, 2.6664+00, 2.5836+00,
    2.4966+00, 2.4047+00, 2.3071+00, 2.2028+00, 2.0901+00,
    1.9666+00, 1.8285+00, 1.6579+00, 1.4652+00,
    1.0163+00

    V331=        0.0000, 1.6421+10, 1.7891+10, 1.9381+10, 2.0892+10,
    2.2425+10, 2.3932+10, 2.5564+10, 2.7172+10, 2.8909+10,
    3.0476+10, 3.2176+10, 3.3909+10, 3.5680+10, 3.7490+10,
    3.9342+10, 4.1243+10, 4.3136+10, 4.5130+10, 4.7240+10,
    4.9357+10, 5.1540+10, 5.3797+10, 5.6132+10, 5.8554+10,
    6.1071+10, 6.3695+10, 6.6435+10, 6.9379+10, 7.2330+10,
    7.5522+10, 7.8911+10, 8.2530+10, 8.6426+10, 9.0670+10,
    9.5353+10, 1.0064+11, 1.0584+11, 1.1473+11,
    1.3225+11

    V431=        4.6947+05, 4.0502+05, 3.9924+05, 3.9338+05, 3.8744+05,
    3.8143+05, 3.7532+05, 3.6913+05, 3.6233+05, 3.5644+05,
    3.4994+05, 3.4332+05, 3.3659+05, 3.2973+05, 3.2274+05,
    3.1562+05, 3.0835+05, 3.0393+05, 2.9336+05, 2.3563+05,
    2.7767+05, 2.6957+05, 2.6125+05, 2.5272+05, 2.4397+05,
    2.3498+05, 2.2573+05, 2.1621+05, 2.0633+05, 1.9623+05,
    1.8572+05, 1.7482+05, 1.6350+05, 1.5171+05, 1.3937+05,
    1.2645+05, 1.1299+05, 9.8725+04, 8.4340+04

```

TABLE 11, EOSTAB INPUT: TITANIUM (Continued)

	7.5075+04
Y5C1=	3.0000 , 4.6931-37, 1.7332-36, 5.2471-35, 1.4013-35, 3.3316-05, 7.1928-05, 1.4313-04, 2.6571-C4, 4.6483-04, 7.7254-04, 1.2282-33, 1.8784-33, 2.7773-33, 3.9862-33, 5.5739-C3, 7.6162-03, 1.0197-02, 1.3407-C2, 1.7344-02, 2.2121-32, 2.7862-32, 3.4590-32, 4.2757-32, 5.2257-02, 6.3361-02, 7.6294-02, 9.1738-02, 1.0280-01, 1.2905-C1, 1.5250-01, 1.8004-31, 2.1719-31, 2.5313-31, 2.9541-31, 3.5091-01, 4.1909-01, 5.0911-01, 6.4012-C1, 1.0163+00
Y6C1=	1.1310+11, 1.2847+11, 1.2975+11, 1.3104+11, 1.3232+11, 1.3360+11, 1.3488+11, 1.3615+11, 1.3743+11, 1.3870+11, 1.3997+11, 1.4123+11, 1.4247+11, 1.4371+11, 1.4493+11, 1.4614+11, 1.4731+11, 1.4847+11, 1.4955+11, 1.5066+11, 1.5172+11, 1.5272+11, 1.5366+11, 1.5455+11, 1.5536+11, 1.5610+11, 1.5674+11, 1.5729+11, 1.5772+11, 1.5802+11, 1.5817+11, 1.5813+11, 1.5739+11, 1.5737+11, 1.5654+11, 1.5528+11, 1.5343+11, 1.5069+11, 1.4E28+11, 1.3225+11
Y7C1=	2.3730+C4, 9.1076+34, 9.4286+04, 9.7543+34, 1.0369+35, 1.0374+05, 1.0669+05, 1.0955+05, 1.1252+C5, 1.1493+C5, 1.1757+35, 1.2034+35, 1.2240+35, 1.2465+35, 1.2676+35, 1.2874+C5, 1.3057+C5, 1.3224+35, 1.3375+C5, 1.3508+C5, 1.3621+05, 1.3715+35, 1.3797+03, 1.3837+35, 1.3862+05, 1.3862+C5, 1.3834+05, 1.3175+35, 1.3684+C5, 1.3558+C5, 1.3392+05, 1.3191+35, 1.2919+05, 1.2599+35, 1.2237+35, 1.1729+C5, 1.1136+05, 1.0186+35, 9.3776+04, 7.5075+04
Y8C1=	1.8770+C6, 2.1174+36,-4.9754+10,-2.6615+35, 1.0943+10, 5.2300+06, 1.1153+11, 4.0000+C1, 0.0000 , 0.0000 , -4.0327+13,-7.7051+13, 3.4799+13,-4.7472+39, 2.7844+38

TABLE 1.2

GRAY EQUATION OF STATE PARAMETERS FOR ALUMINUM

Property	Symbol	Numerical Value
Slope of Hugoniot in shock velocity/ particle velocity space	s	1.338
Lattice gamma at reference volume	γ_o	2.18
Product of ambient specific volume and derivative of lattice gamma with respect to volume	a	1.7
Electronic gamma	γ_e	.6667
Electronic energy coefficient	g_e	$8.7 \times 10^{-9} \frac{\text{Mbar}\cdot\text{cm}^3}{\text{mole}\cdot\text{deg}^2}$
Melting temperature parameter	T_{mo}	1,220 deg
Energy at reference state	E_{OH}	0.
Atomic weight	AW	26.98 gm/mole
Volume at which equations of state are joined	v_J	.474 cm^3/gm
Coefficient of attractive potential for vapor	a_y	47 Mbar (cm^3/mole) ²
Join parameter	θ	1.0
Entropy of melting	DELS	$1.155 \times 10^{-4} \frac{\text{Mbar}\cdot\text{cm}^3}{\text{mole}\cdot\text{deg}}$
Excluded volume for vapor phase	v_b	.1901 cm^3/gm

TABLE 13
GRAY EQUATION OF STATE PARAMETERS FOR BERYLLIUM

Property	Symbol	Numerical Value
Slope of Hugoniot in shock velocity/particle velocity space	s	1.124
Lattice gamma at reference volume	γ_0	1.16
Product of ambient specific volume and derivative of lattice gamma with respect to volume	a	1.0
Electronic gamma	γ_e	.6667
Electronic energy coefficient	g_e	$4.8 \times 10^{-9} \frac{\text{Mbar}\cdot\text{cm}^3}{\text{mole}\cdot\text{deg}}$
Melting temperature parameter	T_m	1,820 deg
Energy at reference state	E_{OH}	0.
Atomic weight	AW	9.01 gm/mole
Volume at which equations of state are joined	V_j	.837 cm^3/gm
Coefficient of attractive potential for vapor	a_y	24 Mbar (cm^3/mole) ²
Join parameter	θ	1.0
Entropy of melting	ΔE_{HS}	$9.55 \times 10^{-5} \frac{\text{Mbar}\cdot\text{cm}^3}{\text{mole}\cdot\text{deg}}$
Excluded volume for vapor phase	V_b	.2645 cm^3/gm

TABLE 15
GRAY EQUATION OF STATE PARAMETERS FOR TITANIUM

Property	Symbol	Numerical Value
Slope of Hugoniot in shock velocity/particle velocity space	s	1.146
Lattice gamma at reference volume	γ_0	1.3
Product of ambient specific volume and derivative of lattice gamma with respect to volume	a	1.1
Electronic gamma	γ_e	.6667
Electronic energy coefficient	g_e	$1.01 \times 10^{-8} \frac{\text{Mbar}\cdot\text{cm}^3}{\text{mole}\cdot\text{deg}}$
Melting temperature parameter	T_{mo}	2,260 deg
Energy at reference state	E_{OH}	0.
Atomic weight	AW	47.9 gm/mole
Volume at which equations of state are joined	v_J	.316 cm^3/gm
Coefficient of attractive potential for vapor	a_y	68 Mbar (cm^3/mole) ²
Join parameter	θ	1.0
Entropy of melting	DELS	$9.637 \times 10^{-5} \frac{\text{Mbar}\cdot\text{cm}^3}{\text{mole}\cdot\text{deg}}$
Excluded volume for vapor phase	v_b	.1281 cm^3/gm

3. RESULTS AND DISCUSSION

The eighteen RIP calculations performed for this research are assigned calculation numbers and described in terms of the equation of state model, the material, and the spectrum in Table 15. The calculated impulses and peak stresses at the end of the source time for aluminum, beryllium, and titanium are presented in Tables 16, 17, and 18 respectively. Note that in most cases the agreement between the three equation of state models is fairly good. It should be noted that the calculated data reveals no obvious trends concerning the tendency for one equation of state to consistently predict stresses and impulses which lie above or below the predictions of the other two models.

TABLE 15
SUMMARY OF RIP CALCULATIONS

Calculation No.	Equation of State	Material	Spectrum
1	EOS1	Aluminum	SPEC 1
2	EOS1	Aluminum	SPEC 2
3	EOS1	Beryllium	SPEC 1
4	EOS1	Beryllium	SPEC 2
5	EOS1	Titanium	SPEC 1
6	EOS1	Titanium	SPEC 2
7	EOS2	Aluminum	SPEC 1
8	EOS2	Aluminum	SPEC 2
9	EOS2	Beryllium	SPEC 1
10	EOS2	Beryllium	SPEC 2
11	EOS2	Titanium	SPEC 1
12	EOS2	Titanium	SPEC 2
13	EOS3	Aluminum	SPEC 1
14	EOS3	Aluminum	SPEC 2
15	EOS3	Beryllium	SPEC 1
16	EOS3	Beryllium	SPEC 2
17	EOS3	Titanium	SPEC 1
18	EOS3	Titanium	SPEC 2

TABLE 16
RESULTS OF RIP CALCULATIONS ON ALUMINUM

Spectrum	Equation of State	Impulse (ktaps)	Peak stress (kbars) at end of source time
SPEC 1	EOS1	293.3	102.5
	EOS2	338.9	104.6
	EOS3	362.8	120.1
SPEC 2	EOS1	4.412	405.5
	EOS2	4.264	427.8
	EOS3	4.357	378.5

TABLE 17
RESULTS OF RIP CALCULATIONS ON BERYLLIUM

Spectrum	Equation of State	Impulse (ktaps)	Peak stress (kbars) at end of source time
SPEC 1	EOS1	105.8	18.48
	EOS2	103.9	22.94
	EOS3	79.51	14.72
SPEC 2	EOS1	36.43	849.7
	EOS2	31.59	943.0
	EOS3	33.31	659.3

TABLE 18
RESULTS OF RIP CALCULATIONS ON TITANIUM

Spectrum	Equation of State	Impulse (ktaps)	Peak stress (kbars) at end of source time
SPEC 1	EOS1	296.8	271.1
	EOS2	252.2	160.4
	EOS3	237.6	183.7
SPEC 2	EOS1	3.809	465.4
	EOS2	3.283	331.3
	EOS3	2.905	338.1

4. CONCLUSIONS AND RECOMMENDATIONS

The modified PUFF equation of state is easy to use and gives results which are comparable to the more sophisticated models; this feature of course is the primary reason that modified PUFF is so widely applied in hydrodynamic calculations. However, this model has several disadvantages which are inherent due to its simplicity:

1. It is highly empirical and is therefore dependent on UGT or electron beam generated data.
2. The melting and vaporization phase transitions are described by energy levels which have no volume (or pressure) dependence.
3. The model contains no explicit caloric equation of state; the temperature, which may be required for some applications, is therefore unknown.

The RIP mixed phase equation of state was developed in order to partially relax the above restrictions. However, we find that additional work is required before that model can be considered a useful calculational tool. The following improvements are recommended:

1. The lowest temperature-volume point on the mixed phase boundary (see Figure 3) should be the boiling point at ambient pressure, i.e., $\theta = \theta_b$, the boiling temperature and $V = V_b$, the specific volume at the boiling temperature.
2. The join function should extend from the ambient volume, V_o , to the boiling volume, V_b (see Figure 3). Thus the join function will not penetrate the mixed phase region causing the discontinuities which exist in the present RIP mixed phase equation of state.

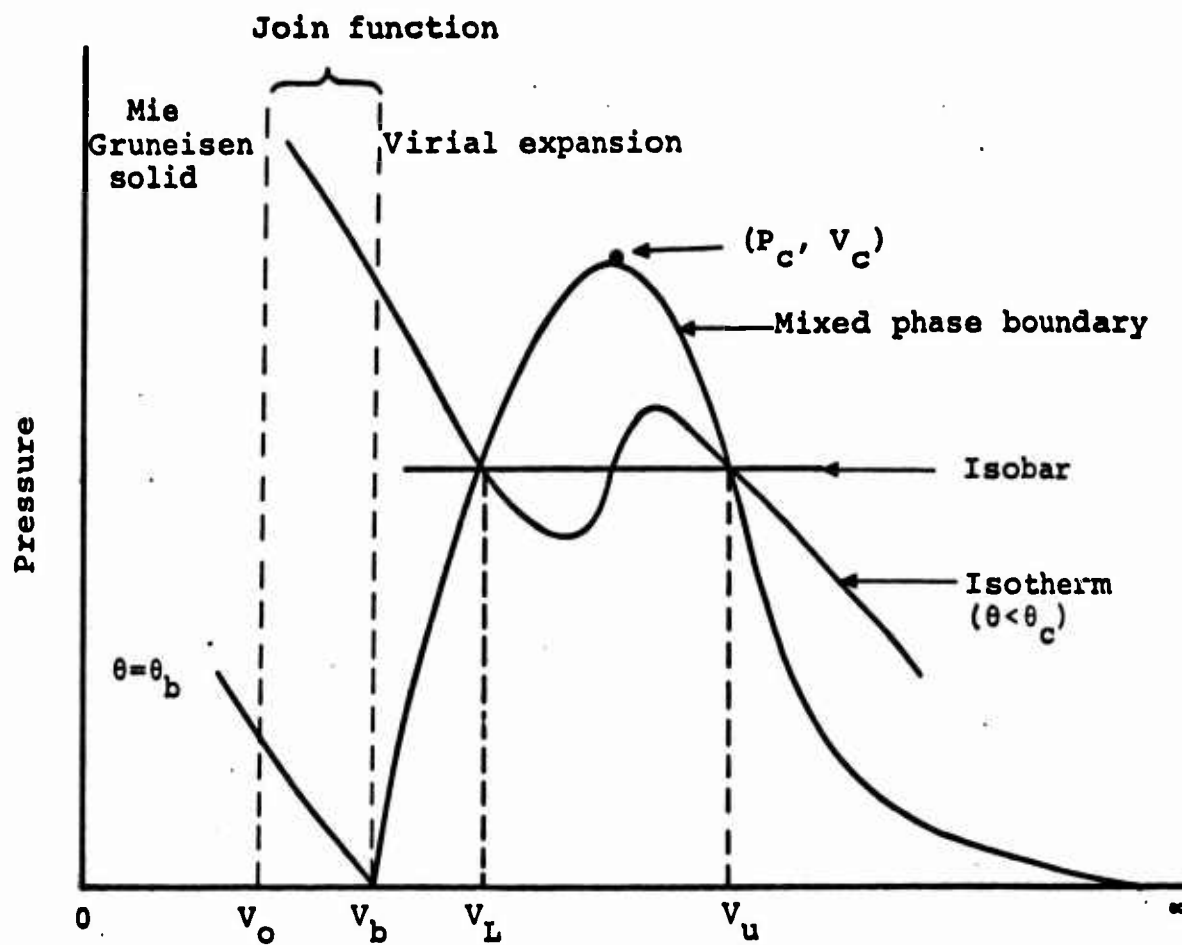


Figure 3. Intersection of isotherms with mixed phase boundary.

3. The EOSGEN code should be incorporated into the RIP code as a subroutine which is called after the initial call to the EOS2 subroutine; this would eliminate the need to perform a separate calculation with the EOSGEN code and would greatly simplify data input for the RIP mixed phase equation of state.

The GRAY equation of state contains the most sophisticated equation of state models available in the RIP code. However, the procedure used to join the Grover liquid equation of state and the Young-Alder model destroys the physical significance of the Young-Alder model, particularly in the liquid-vapor region. Additionally, since the join volume used in the GRAY equation of state is too large, the Grover model is applied in regions where its accuracy is highly questionable.

The procedure we recommend for correcting these deficiencies is best explained in terms of a pressure-volume diagram which is presented schematically in Figure 4. The reference or ambient condition is assumed to be

$$P = P_0 \approx 0, \text{ pressure}$$

$$T = T_0, \text{ temperature}$$

and $V = V_0, \text{ specific volume}$

The specific volumes indicated on the abscissa are:

V_{mo} = reference pressure intercept of solidus

V_{Lo} = reference pressure intercept of liquidus

V_{bo} = reference pressure intercept of liquid-vapor phase boundary.

V_c = critical specific volume

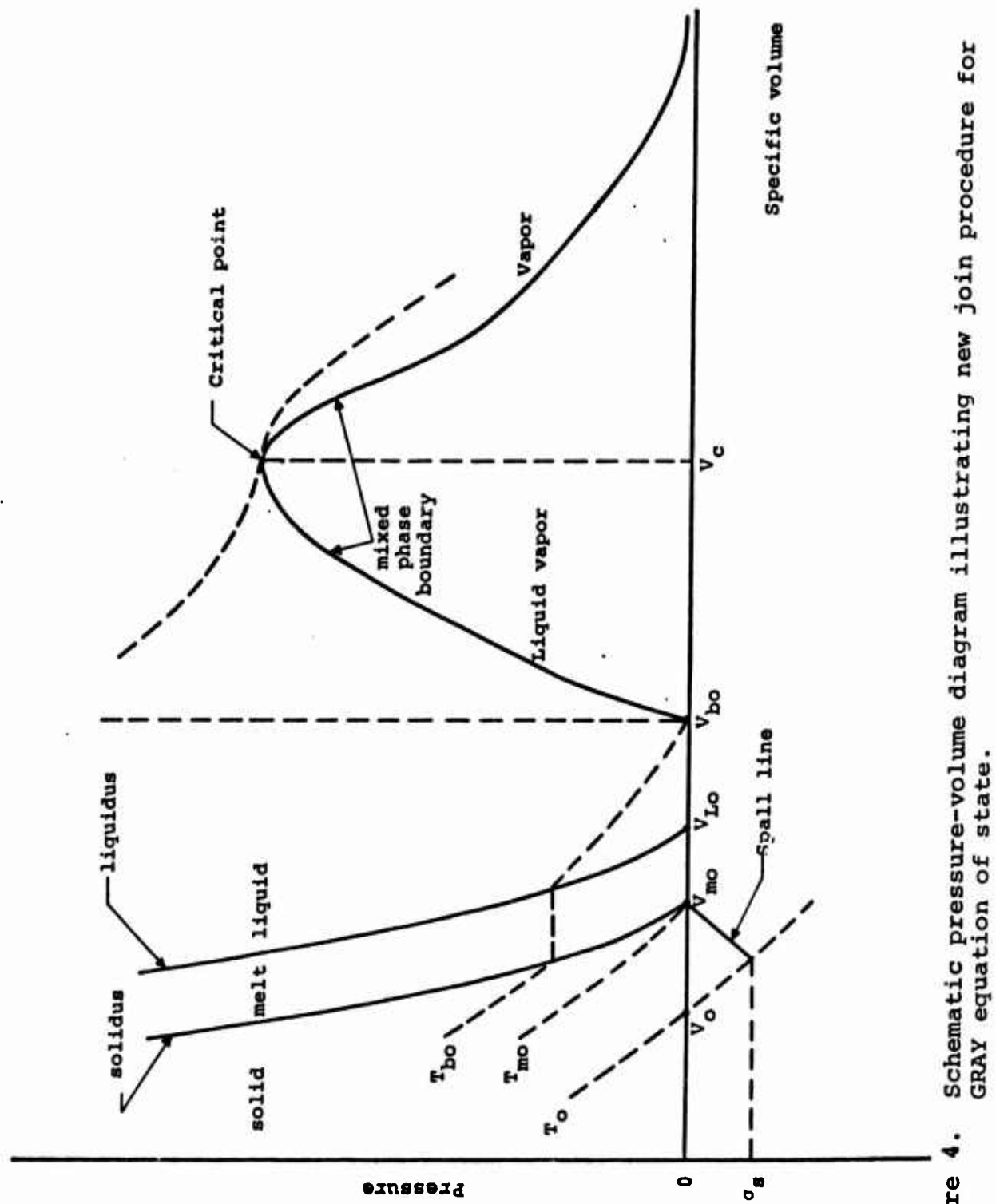


Figure 4. Schematic pressure-volume diagram illustrating new join procedure for GRAY equation of state.

Isotherms passing through the reference pressure at V_o , V_{mo} , V_{bo} and V_c are denoted by T_o , T_{mo} , T_{bo} and T_c respectively. The basic problem with the GRAY equation of state is that the join volume lies to the right of V_{bo} in Figure 4; thus the Young-Alder isotherms in the liquid-vapor region are badly distorted. Consequently, no attempt was made to perform a Maxwell construction in order to identify the liquid-vapor phase boundary; failure to perform this construction results in the appearance of unstable states to the right of the join volume due to loops in the Gibbs free energy along isotherms. We therefore recommend that the Grover and Young-Alder models be joined at some locus between the liquidus and V_{bo} , the specific volume at the reference pressure and the boiling temperature. Joining the two models in this region will leave the Young-Alder model in tact and allow one to perform the Maxwell construction. One of several methods may be used to join the Grover and Young Alder models:

1. The models could be joined at the locus of intersection of corresponding isotherms if that locus does not lie within the mixed phase region.
2. The two models could be joined by a fairing function applied between V_{Lo} and V_{bo} .
3. A fairing function may be applied to the entire region between the liquidus and V_{bo} .

It should be emphasized that the recommended changes to the GRAY equation of state are very important because they will make it possible to determine all phase transitions explicitly; this capability is especially desirable for applications involving the x-ray induced response of porous materials. A recent study performed at Lawrence Livermore Laboratory[11] shows that impulse production in porous materials occurs on two distinct time scales. The short time contribution, which occurs in less than a microsecond, is due to pore closure by thermal expansion which results in high pressures and substantial blow-off velocities. The second contribution, which occurs over a time period of tens of microseconds, is due to the vapor pressure in the mixed liquid/vapor region. The vapor pressure tends to accelerate the material in front of it (either blowoff material or material in the missile structure which acts as a tamper) over a long time period and can result in a significant contribution to the total impulse.*

* It should be mentioned that explicit identification of phase boundaries is also important with respect to laser induced material response because it would enable one to identify regions in which liquid droplets are present. Liquid droplets can drastically affect the optical properties of the medium and these properties are, of course, quite important for predicting laser interactions.

REFERENCES

1. R.H. Fisher and H.E. Read, "RIP, A One-Dimensional Material Response Code", Systems, Science and Software Report SSS-R-72-1324, September 1972.
2. D.R. Tuerpe, R.N. Keeler and S.L. McCarthy, "The Volumetric Properties and Electrical Conductivity of Aluminum at High Temperature and Pressures", Lawrence Livermore Laboratory Report UCID-4683, January 1964.
3. E.B. Royce, "GRAY, A Three-Phase Equation of State for Metals", Lawrence Livermore Laboratory, UCRL-51121, September 1971.
4. R. Grover, "Liquid Metal Equation of State Based on Scaling", J. Chem. Phys., 55, 3435 (1971).
5. R.N. Keeler and E.B. Royce, "Shock Waves in Condensed Media", p. 51 ff. in Physics of High Energy Density, P. Caldirola and N. Knopfel, eds. (Academic Press, New York, 1971); Lawrence Livermore Laboratory Report UCRL-71846 (1969).
6. D.A. Young and B.J. Alder, "Critical Point of Metals from the van der Waals Model", Phys. Rev. A3, 364, 1971.
7. Private communication with Janet Lacetera, Effects Analysis Branch, Ballistic Research Laboratory, Aberdeen, Maryland, 25 June 1973.
8. Brian J. Kohn, "Compilation of Hugoniot Equations of State", Air Force Weapons Laboratory, AFWL-TR-69-38, April 1969.
9. Robert C. Weast, Handbook of Chemistry and Physics, The Chemical Rubber Company, Cleveland, Ohio, May 1968, pages D-33, D-34, D-97 and D-103.
10. D.R. Stull and G.C. Sinke, Thermodynamic Properties of the Elements, American Chemical Society, Washington, D.C., 1965.
11. John J. Ruminer, "Liquid/Vapor Contributions to Impulse from Porous Materials", Lawrence Livermore Laboratory, UCRL-51354, February 21, 1973.

APPENDIX A
THE EOSGEN CODE

Three tasks are performed by the EOSGEN code: 1) Evaluation of the seven coefficients in the virial expansion, 2) definition of the mixed phase boundary, 3) evaluation of the seven coefficients in the join function. These tasks are discussed separately in the following sections of this Appendix.

A.1 THE VIRIAL EXPANSION

The virial expansion employed by the RIP mixed phase equation of state, with density and energy as independent variables, is

$$P = \frac{(z_1 \rho + z_2 \rho^2 + z_4 \rho^3)_E}{z_6} + z_{11} \rho + z_{12} \rho^2 + z_{13} \rho^3 + z_{14} \rho^4 + z_{15} \rho^5 , \quad (1)$$

where

$$R(\theta_o) = \frac{3P_c V_c \theta_o}{\theta_c}$$

$$z_1 = \frac{3P_c V_c}{\theta_c}$$

$$z_2 = \frac{-3P_c V_c^2 + V_o [\beta_o V_o + 2R(\theta_o)]}{\theta_c - \theta_o}$$

$$z_3 = \frac{-V_o \theta_c [\beta_o V_o + 2R(\theta_o)] + 3P_c V_c^2 \theta_o}{\theta_c - \theta_o}$$

$$z_4 = \frac{P_c V_c^3 - V_o^2 [\beta_o V_o + R(\theta_o)]}{\theta_c - \theta_o} .$$

$$z_5 = \frac{V_o^2 \theta_c [\beta_o V_o + R(\theta_o)] - P_c V_c^3 \theta_o}{\theta_c - \theta_o}$$

$$z_6 = c_{v_o}$$

$$z_7 = - \left[\frac{z_3}{V_o} + \frac{z_5}{2V_o^2} + z_6 \theta_c \right]$$

$$z_{11} = -z_1 \left(\frac{z_7}{z_6} \right)$$

$$z_{12} = -z_1 \left(\frac{z_3}{z_6} \right) - z_2 \left(\frac{z_7}{z_6} \right) + z_3$$

$$z_{13} = - \frac{z_1}{2} \left(\frac{z_5}{z_6} \right) - z_2 \left(\frac{z_3}{z_6} \right) - z_4 \left(\frac{z_7}{z_6} \right) + z_5$$

$$z_{14} = - \frac{z_2}{2} \left(\frac{z_5}{z_6} \right) - z_4 \left(\frac{z_3}{z_6} \right)$$

$$z_{15} = - \frac{z_4}{2} \left(\frac{z_5}{z_6} \right) .$$

In Equation (1), P is the pressure, ρ is the density and E is the energy. The coefficients, z_i , are expressed in terms of the critical and reference point characteristics presented in Tables 4, 5 and 6. The coefficients z_1 through z_7 are evaluated by the EOSGEN code and must be read into the first

seven locations of the Z array in EOSTAB common in the RIP code. The coefficients z₁₁ through z₁₅ are evaluated by subroutine EOS2 in the RIP code and need not be input.

A.2 DEFINITION OF THE MIXED PHASE BOUNDARY

Corresponding values of pressure, density, energy and sound speed on the mixed phase boundary are required as input for the RIP mixed phase equation of state. These data are determined by locating points having equal pressure and Gibbs free energy on a series of isotherms between the reference temperature, θ_0 , and the critical temperature θ_c . Referring to the schematic pressure/volume diagram presented in Figure A.1, the two points on the mixed phase boundary of an isotherm with temperature, $\theta_0 < \theta < \theta_c$, are determined by the following equalities:

$$P_u(\theta, \rho_u) = P_L(\theta, \rho_L) , \quad (2)$$

$$G_u(\theta, \rho_u) = G_L(\theta, \rho_L) , \quad (3)$$

where G is the Gibbs free energy, P is the pressure and ρ_L and ρ_u are densities on the low and high density sides of the mixed phase boundary respectively. The pressure, as a function of density and temperature, is given by

$$P(\rho, \theta) = z_1\theta\rho + (z_2\theta + z_3)\rho^2 + (z_4\theta + z_5)\rho^3 , \quad (4)$$

and the Gibbs free energy is defined as

$$G = E + PV - \theta S ,$$

where E is the specific energy and S is entropy. Taking the differential of the Gibbs free energy yields

$$dG = dE + PdV + VdP - \theta dS - Sd\theta ,$$

which reduces to

$$dG = VdP , \quad (5)$$

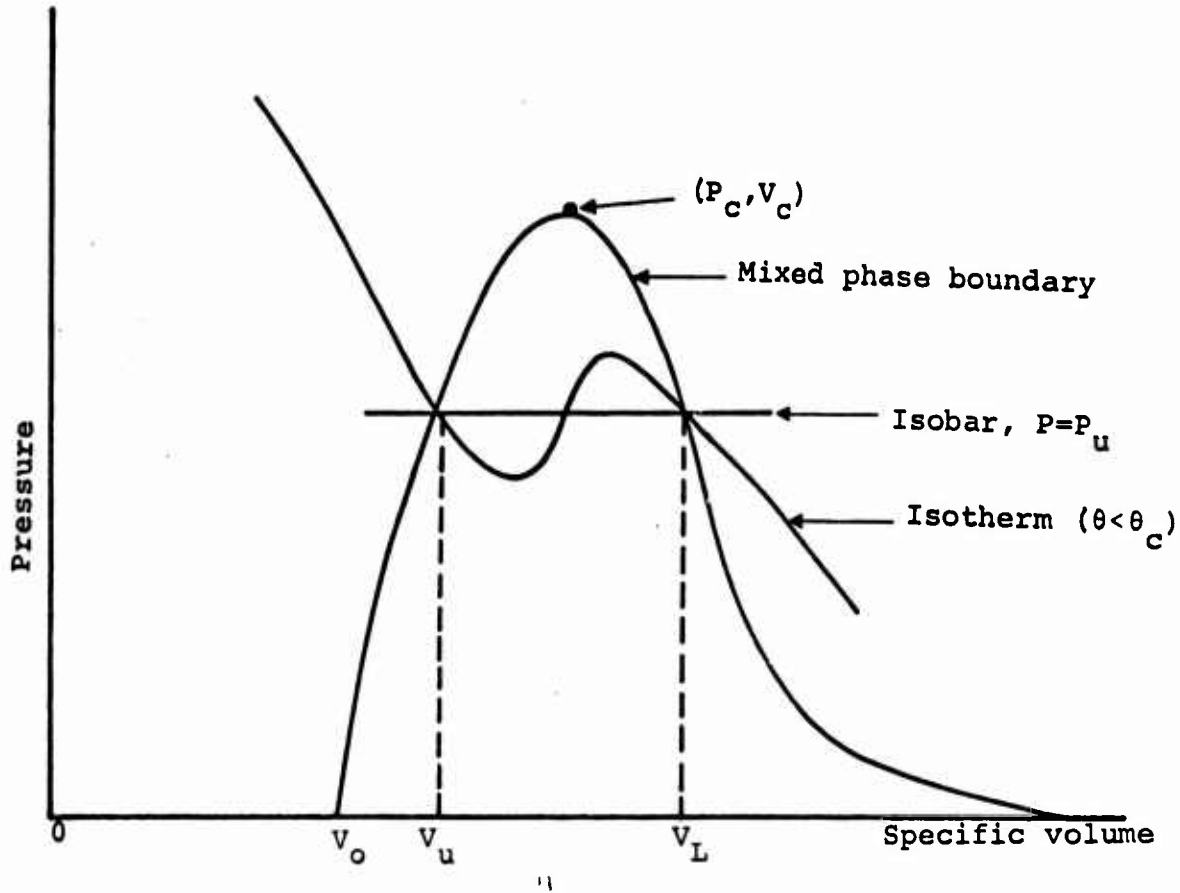


Figure A.1 Intersection of isotherms with mixed phase boundary.
 (Note: $\rho_L = 1/v_L$; $\rho_u = 1/v_u$).

for an isothermal process. Therefore, the Gibbs free energy, referenced to the initial density, is

$$G(\theta, \rho) = \int_{1/\rho_0}^{1/\rho} V dP = \int_{1/\rho_0}^{1/\rho} V \left(\frac{\partial P}{\partial V} \right)_\theta dV . \quad (6)$$

Substituting Equation (4) into the above relation and performing the indicated integration yields

$$G(\theta, \rho) = -z_1 \theta \ln \left(\frac{\rho_0}{\rho} \right) + (2\theta z_2 + z_3)(\rho - \rho_0) + \frac{3}{2} (z_4 \theta + z_5) (\rho^2 - \rho_0^2) . \quad (7)$$

Now, Equations (4) and (7) are substituted into Equation (2) and (3) respectively, and the quantities P_u , ρ_u and ρ_L are calculated by a numerical iteration scheme in the EOSGEN code. The specific energies on the mixed phase boundary are determined by

$$E_u = E(\theta, \rho_u) ,$$

and

$$E_L = E(\theta, \rho_L) ,$$

where

$$E = z_3 \rho + \frac{z_5}{2} \rho^2 + z_6 \theta + z_7 ,$$

is the caloric equation of state employed in the expanded region of the RIP mixed phase equation of state. The sound speeds on the mixed phase boundary are given by

$$c_u = \sqrt{\left(\frac{\partial P}{\partial \rho} \right)_S} \quad \text{evaluated at } \theta \text{ and } \rho = \rho_u$$

$$c_L = \sqrt{\left(\frac{\partial P}{\partial \rho}\right)_S} \quad \text{evaluated at } \theta \text{ and } \rho = \rho_L .$$

The quantities on the mixed phase boundary are stored in the following arrays in EOSTAB common in the RIP code:

$\theta \rightarrow \text{THETA}(I)$

$P_u \rightarrow PU(I)$

$\rho_u \rightarrow RHO_U(I)$

$E_u \rightarrow EU(I)$

$c_u \rightarrow CU(I)$

$\rho_L \rightarrow RHOL(I)$

$E_L \rightarrow EL(I)$

$c_L \rightarrow CL(I) .$

The number of data points to be stored in each of the above arrays must be input to Z(8) of the Z(I) array which is also in EOSTAB common.

A.3 THE JOIN FUNCTION

The purpose of the join function is to allow pressure and sound speed continuity between the Mie Gruneisen solid equation of state for the compressed region and the virial expansion for the expanded region. The join function is applied over a density range beginning at the ambient density, ρ_0 , and ending at a slightly expanded cut-off density of ρ_{co} (see Figure A.2). It was determined that in general it is possible for the join function originally reported in Reference 1 to contain several singularities over this density range; in fact, these singularities appeared when the calculations performed for this report were first attempted. We therefore decided to develop a new join function which would not exhibit singularities under any conditions.

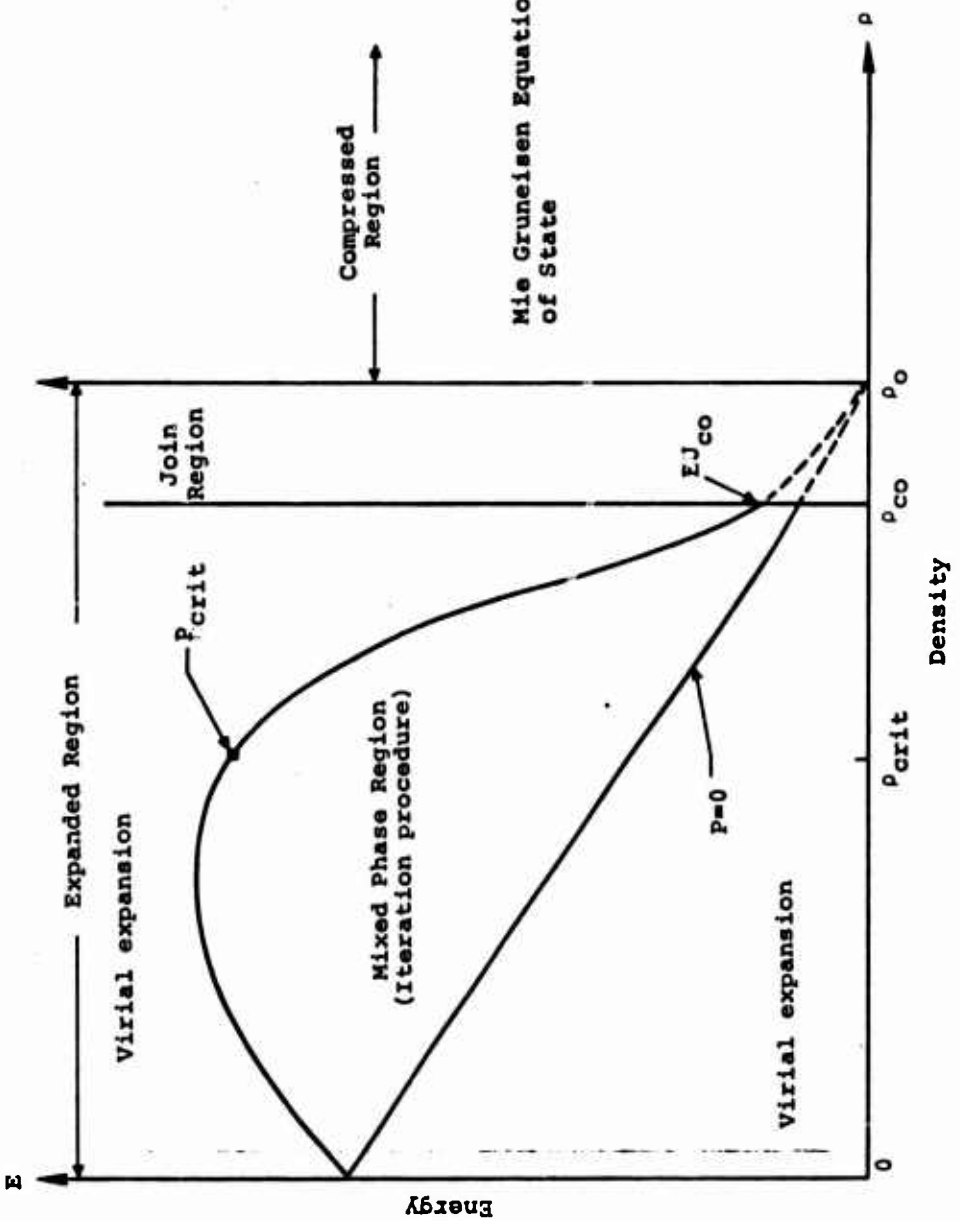


Figure A.2 Schematic representation of the RIP mixed phase equation of state.

The new join function developed for this series of calculations is:

$$P_2 = \left[c_5 + c_6 \left(\frac{\rho_o - \rho}{\rho_o - \rho_{oc}} \right)^2 + c_7 \left(\frac{\rho_o - \rho}{\rho_o - \rho_{oc}} \right)^3 \right] E + c_1 + c_2 \rho + c_3 \rho^2 + c_4 \rho^3 , \quad (7)$$

where P_2 is the pressure and the subscript, 2, serves to identify the join function. The seven coefficients, $c_1 \dots c_7$, are determined by continuity conditions at the ambient and cut-off densities. Letting the subscripts 1 and 3 represent the Mie Gruneisen solid equation of state and the virial expansion respectively, we have

$$P_1 = G_o \rho_o E + (A_1 \mu + A_2 \mu^2 + A_3 \mu^3) \left(1 - \frac{G \mu}{2} \right) , \quad (8)$$

where

$$\mu = \frac{\rho}{\rho_o} - 1 ,$$

$$P_3 = \frac{z_1 \rho + z_2 \rho^2 + z_4 \rho^3}{z_6} E + z_{11} \rho + z_{12} \rho^2 + z_{13} \rho^3 + z_{14} \rho^4 + z_{15} \rho^5 . \quad (9)$$

The appropriate boundary conditions for determining the coefficients in the join function are:

$$P_1(\rho_o, E) = P_2(\rho_o, E) \quad (10)$$

$$\left. \frac{\partial P_1}{\partial \rho} \right|_E = \left. \frac{\partial P_2}{\partial \rho} \right|_E \quad \text{at } \rho = \rho_o \quad (11)$$

$$\left. \frac{\partial P_1}{\partial E} \right|_{\rho} = \left. \frac{\partial P_2}{\partial E} \right|_{\rho} \quad \text{at } \rho = \rho_o \quad , \quad (12)$$

$$P_2(\rho_{co}, E) = P_3(\rho_{co}, E) \quad , \quad (13)$$

$$\left. \frac{\partial P_2}{\partial \rho} \right|_E = \left. \frac{\partial P_3}{\partial \rho} \right|_E \quad \text{at } \rho = \rho_{co} \quad , \quad (14)$$

$$\left. \frac{\partial P_2}{\partial E} \right|_{\rho} = \left. \frac{\partial P_3}{\partial E} \right|_{\rho} \quad \text{at } \rho = \rho_{co} \quad . \quad (15)$$

Substituting Equations (7), (8), and (9) into boundary conditions (10) through (15) yields the following set of independent equations for the undetermined coefficients in the join function.

$$c_5 = N_1 \quad (16)$$

$$c_5 + c_6 + c_7 = N_4 \quad (17)$$

$$\frac{2}{\rho_o - \rho_{co}} c_6 + \frac{3}{\rho_o - \rho_{oc}} c_7 = -N_6 \quad (18)$$

$$c_1 + c_2 \rho_o + c_3 \rho_o^2 + c_4 \rho_o^3 = 0 \quad (19)$$

$$c_2 \rho_o + 2c_3 \rho_o^2 + 3c_4 \rho_o^3 = N_2 \quad (20)$$

$$c_1 + c_2 \rho_{co} + c_3 \rho_{co}^2 + c_4 \rho_{co}^3 = N_3 \quad (21)$$

$$c_2 + 2c_3 \rho_{co} + 3c_4 \rho_{co}^2 = N_5 \quad (22)$$

where

$$N_1 = \rho_o G_o$$

$$N_2 = A_1$$

$$N_3 = z_{11}\rho_{co} + z_{12}\rho_{co}^2 + z_{13}\rho_{co}^3 + z_{14}\rho_{co}^4 + z_{15}\rho_{co}^5$$

$$N_4 = \frac{z_1\rho_{co} + z_2\rho_{co}^2 + z_4\rho_{co}^3}{z_6}$$

$$N_5 = z_{11} + 2z_{12}\rho_{co} + 3z_{13}\rho_{co}^2 + 4z_{14}\rho_{co}^3 + 5z_{15}\rho_{co}^4$$

$$N_6 = \frac{z_1 + 2z_2\rho_{co} + 3z_4\rho_{co}^2}{z_6} .$$

Equations (16) through (21) are easily solved by Cramer's rule; the task is performed by the EOSGEN code. Additionally, the cut-off density, ρ_{co} , is selected automatically by the EOSGEN code based on the following considerations:

1. The coefficient of E in Equation (9) has a value at $\rho = \rho_{co}$ which is less than the coefficient of E in Equation (8).
2. The remaining terms in Equation (9) have a negative value at $\rho = \rho_{co}$ and their derivative has a positive value at $\rho = \rho_{co}$.

The new join function discussed in the above paragraphs is mathematically cleaner (no singularities) and greatly facilitates application of the RIP Mixed Phase equation of state.

APPENDIX B

CORRECTIONS TO EOS2

Two types of corrections to subroutine EOS2 (the RIP mixed phase equation of state) were required in order to perform the calculations presented in this report. The first set of corrections are related to the incorporation of the new join function (see Appendix A.3) into subroutine EOS2. The second correction is a temporary measure designed to compensate for inherent discontinuities in the RIP mixed phase equation of state. These discontinuities exist between the mixed phase region and the virial expansion region below the zero pressure line in Figure B.1; the mixed phase and virial expansion regions in question are denoted as 27 and 26, respectively, in the same figure. The task of correcting the discontinuity in a thermodynamically consistent manner is beyond the scope and intent of this program; however, a temporary correction was required in order to avoid numerical convergence problems encountered when a Lagrangian cell attempted to follow a path from the 26 region to the 27 region. Since such a transition is discontinuous and physically meaningless and because convergence problems were encountered whenever such a transition occurred, it was decided to artificially forbid it with appropriate modifications to the EOS2 subroutine.

A FORTRAN listing which details the required corrections to the EOS2 subroutine in the RIP code is presented at the end of this appendix.

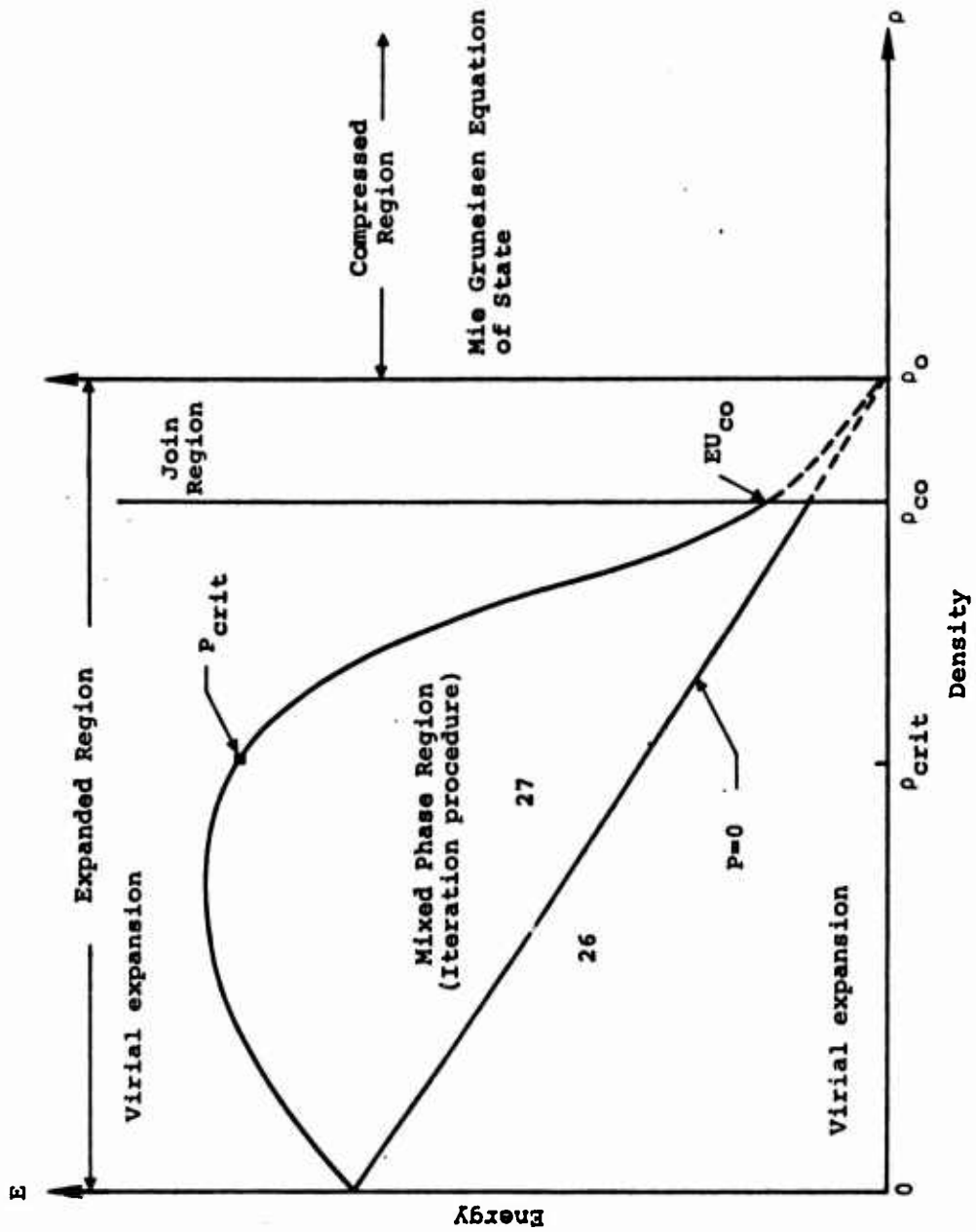


Figure B.1 Schematic representation of the RIP mixed phase equation of state.

THE FOLLOWING CHANGES TO EOS2 (RIP MIXED PHASE EQUATION OF STATE) ARE REQUIRED IN THE EXISTING MODEL IN ORDER TO INCORPORATE THE JOIN FUNCTION AND TO COMPENSATE FOR DISCONTINUITIES BETWEEN THE MIXED PHASE REGION AND THE VIRIAL EXPANSION REGION BELOW THE ZERO PRESSURE LINE.

1. IN THE CODING WHICH FOLLOWS *** POINT IS IN MIXED PHASE REGION *** COMMENT CARD ADD THE FOLLOWING LINES AFTER THE LINE WHICH STATES:

```
TEMP(11)=PU(NMAX)
```

ADD LINES:

```
IF(TEMP(1) .GT. TEMP(10)) GO TO 155  
P(J)=TEMP(10)  
IVFLAG(J)=26  
C(J)=ESTCON(6,N)  
GO TO 260
```

AND CHANGE THE STATEMENT WHICH STATES:

```
IF(TEMP(1) .GT. TEMP(11)) TEMP(1)=TEMP(11)
```

TO THE FOLLOWING:

```
155 IF(TEMP(1) .GT. TEMP(11)) TEMP(1)=TEMP(11)
```

2. AFTER THE LINE OF CODING,

```
250 IVFLAG(J)=25
```

THE FOLLOWING LINES HAVE BEEN DELETED AND REPLACED:

```
TEMP(2)=COS(ESTCON(22,N)*TEMP(1))  
TEMP(3)=ESTCON(21,N)/TEMP(2)+ESTCON(23,N)  
TEMP(4)=SIN(TEMP(1))  
TEMP(5)=ESTCON(21,N)*ESTCON(22,N)*TEMP(4)/((ESTCON(1,N)-ESTCON(16,  
N))*TEMP(2)**2)
```

THE NEW LINES SHOULD READ:

```
TEMP(2)=TEMP(1)**2  
TEMP(3)=ESTCON(23,N)+TEMP(2)*(ESTCON(21,N)+ESTCON(22,N)+TEMP(1))  
TEMP(5)=-(2.*ESTCON(21,N)*TEMP(1)+3.*ESTCON(22,N)*TEMP(2))/  
*(ESTCON(1,N)-ESTCON(16,N))
```

APPENDIX C
CORRECTIONS TO EOS3

Two coding errors were discovered in the expression for temperature in the liquid-vapor region of the GRAY equation of state. The FORTRAN changes required to correct these errors are presented in the listing at the end of this appendix.

Due to the lack of continuity between the liquid vapor region and the liquid, melt, and solid regions (see Figure C.1) problems (complex temperatures) were encountered whenever Lagrangian cells attempted to cross the boundary between them; this problem is inherent to the GRAY equation of state because the liquid-vapor region is continuous only with the hot liquid region. The task of providing complete continuity in this equation of state is beyond the scope and intent of this project. Therefore, temporary FORTRAN changes were incorporated into the EOS3 and EOS subroutines which prevent the liquid-vapor region from being entered by any path not leaving the hot liquid region. These changes are detailed in the FORTRAN listing which follows.

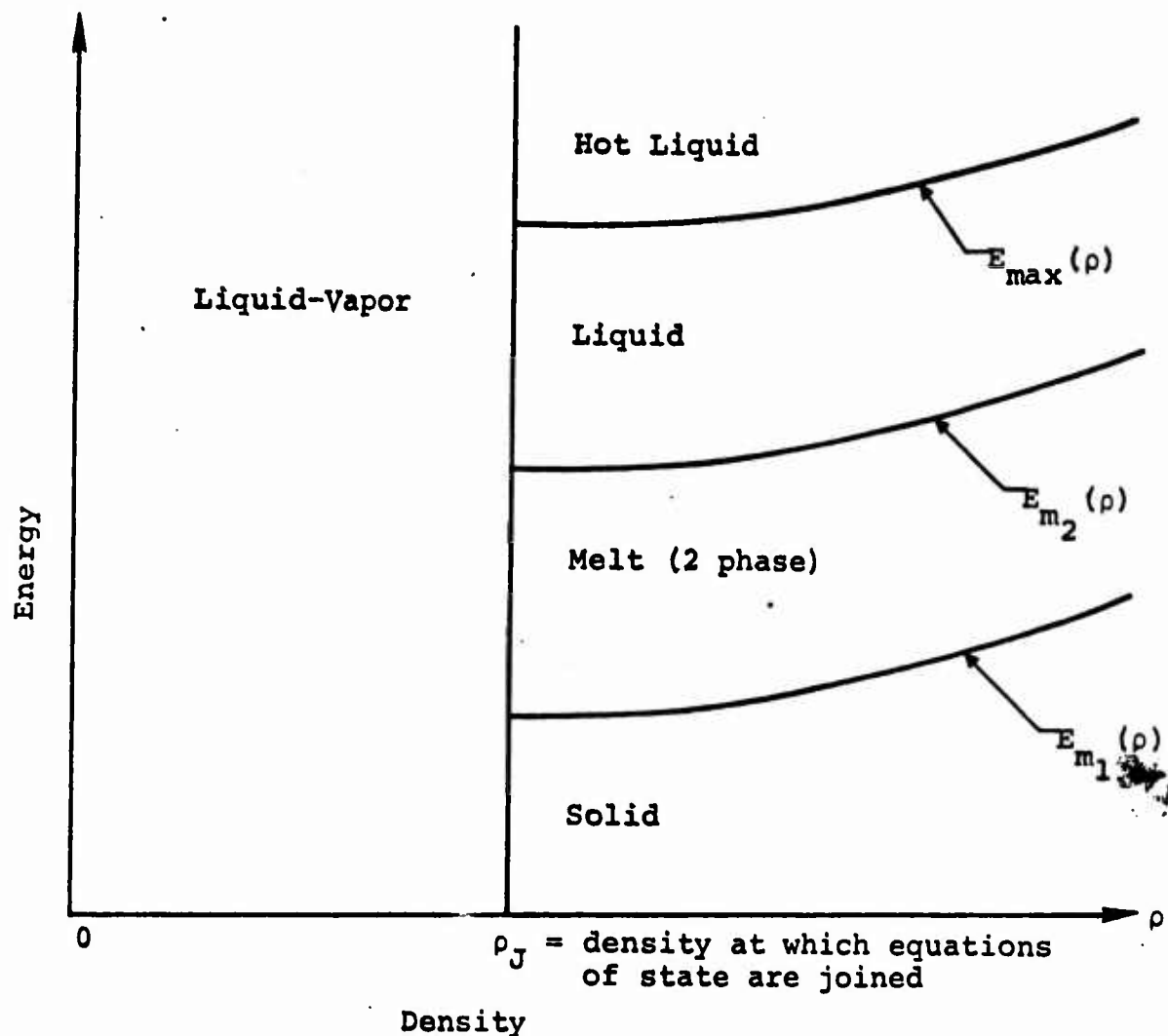


Figure C.1 Schematic representation of GRAY EOS.

THE FOLLOWING CHANGES TO EOS AND EOS3 (GRAY EQUATION OF STATE) SUBROUTINES ARE REQUIRED IN THE EXISTING MODELS.

A. SUBROUTINE EOS

1. IN THE SECTION OF CODING FOLLOWING THE COMMENT STATEMENT *** LRL EOS *** ADD TWO LINES AFTER THE ONE WHICH STATES:

30 RSAVE=RHO(J)

ADDED LINES:

```
PSAVE2=P(J)
ISAVE=IVFLAG(J)
```

ALSO IN THIS SAVE SECTION TWO LINES ARE ADDED IMMEDIATELY FOLLOWING THE LINE STATING:

PSAVE=P(J)

ADDED LINES:

```
IVFLAG(J)=ISAVE
P(J)=PSAVE2
```

B. SUBROUTINE EOS3

1. IN THE SECTION OF CODING FOLLOWING THE COMMENT STATEMENT *** VAPOR REGION *** ADD SIX LINES OF CODING BETWEEN THE COMMENT STATEMENT AND THE LINE WHICH READS:

90 IVFLAG(J)=35

```
90 IF(IVFLAG(J) .GE. 33) GO TO 85
    P(J)=0.
    GO TO 100
85 IF(P(J) .GT. 1.E-12) GO TO 86
    P(J)=0.
    GO TO 100
```

AND CHANGE THE LINE OF CODING WHICH READS:

90 IVFLAG(J)=35

TO READ:

86 IVFLAG(J)=35

ALSO, IN THE SAME SECTION OF CODING CHANGE THE STATEMENT WHICH STATES:

```
TEMP(7)=-{E(J)+ECON(17,N)*TEMP(1)/ESTCON(26,N)-ECON(4,N)*TEMP(6)-
•          ECON(10,N)}
```

TO THE FOLLOWING:

```
TEMP(7)=-{E(J)+ECON(17,N)*TEMP(1)/ESTCON(26,N)
I           -ECON(14,N)*TEMP(6)-ECON(10,N)*2}
```

AND ADD THE FOLLOWING 15 LINES.

```
T1234=TEMP(5)**2-2-*TEMP(4)*TEMP(7)
IF(T1234 .GT. 0) GO TO 92
PRINT 91,ECON(5,N),ECON(10,N),ECON(11,N),ECON(12,N),ECON(14,N),
I   ECON(15,N),ECON(16,N),ECON(17,N),TEMP(6)
91 FORMAT(5X,9HPRIME = ,E12.3,//,
1      5X,SHD1 = ,E12.3,//,
2      5X,SHD2 = ,E12.3,//,
3      5X,SHD3 = ,E12.3,//,
4      5X,SHC1 = ,E12.3,//,
5      5X,SHC2 = ,E12.3,//,
6      5X,SHC3 = ,E12.3,//,
7      5X,10HAYPRIME = ,E12.3,//,
8      5X,SHFE = ,E12.3,//)
CALL SPRINT (6HE0S3 ,6HLRR0R9)
92 CONTINUE
```